The Plattenkalk Unit in the Talea Ori Mountains - Sisses Traverse

Stromatolite marble bed within the Platy Marble Unit. This part of the Unit is also known as the Mavri Formation and belongs to the Talea Ori-Group

By George Lindemann, MSc.

Berlin, October 2023

Contents

Appendix

1 Introduction to the Talea Ori-Group

The Talea Ori-Group consists mainly of carbonate rocks from the shelf and deeper shelf areas. At the top of the stratigraphic sequence, the Aloides Formation is the thickest of the various formations within the Talea Ori-Group. It contains white chert nodules and layers, which is a characteristic feature of the Aloides Formation and often comes to mind when dealing with the "Plattenkalk". The Aloides Formation makes up a large part of the central mountain ranges on Crete e.g. the Ida Ori and Lefka Ori mountains. However, within the Talea Ori Mts. the lower formations are quite unique to that area and are therefore called the Talea Ori-Group. The sequence of predominantly carbonate rocks begins with the Fodele Formation, the basal part of which consists of the Galinos shales. The Fodele Formation is overlain by the Sissi Formation followed by the Mavri Formation. The time line within the Talea Ori section begins approx. at the Upper Carboniferous and extends to the Liassic and Eocene.

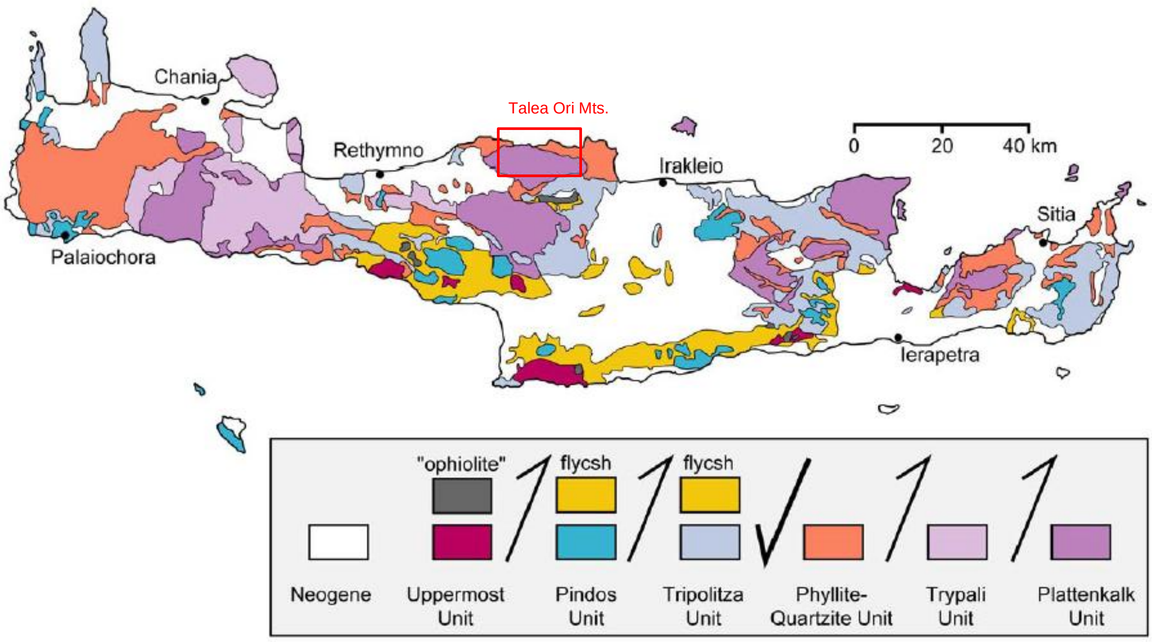

Simplified geologic map of Crete showing the remains of the different nappes. Arrows within the legend indicate major thrust planes. The bold arrow represents the Cretan Detachment. After Creutzburg et al. (1977) and Thomson et al. (1999). [J. M. Rahl et. al., 2004]

The Talea Ori-Group structurally underlies the Phyllite–Quartzite unit s. str. (see My GeoGuide No. 26: The Phyllite-Quartzite Unit Talea Ori Mountains West of Heraklion). The Talea Ori group, which is tectonically sometimes referred to as the "para-autochthone", underwent subduction related high-pressure low-temperature (HP-LT) metamorphism and therefore must be allochthonous (Theye et al. 1992). The Plattenkalk unit is considered the most external and lowermost unit of the Hellenides. The basement is not exposed (Krahl et al. 1988). The External Hellenides comprise several tectonic nappes that were stacked during the Alpine Mountain building phase (see figure above). The lower nappes, which encompasses the Phyllite-Quartzite unit and the Plattenkalk unit including the lower part of the Talea Ori group underwent subduction in Late Oligocene to Miocene times and were rapidly exhumed (Thomson et al. 1998). The Talea Ori group and the Phyllite-Quartzite Unit s. str. were stacked side by side during mountain building at peak metamorphic temperatures and experienced a similar tectonometamorphic history. A later phase of deformation was constituted by an extensional shear zone arising from updoming related exhumation of the HP-LT metamorphic rocks (e.g. Thomson et al. 1999, Seybold et al. 2019). Based on to the general nappe character of the Talea Ori group and the Phyllite-Quartzite Unit s. str. the tectonic contact between the two units is commonly described as a thrust fault (Chatzaras et al. 2006; Xypolias et al., 2007) although other authors regard the contact to resemble a normal fault (Richter & Kopp, 1983).

Near the village of Sisses the Talea Ori Group is part of an overturned limb of a south-vergent fold – it is therefore structurally inverted (see Figure c, Seybold et al. 2019). The following text describes each Formation beginning at the base of the sequence.

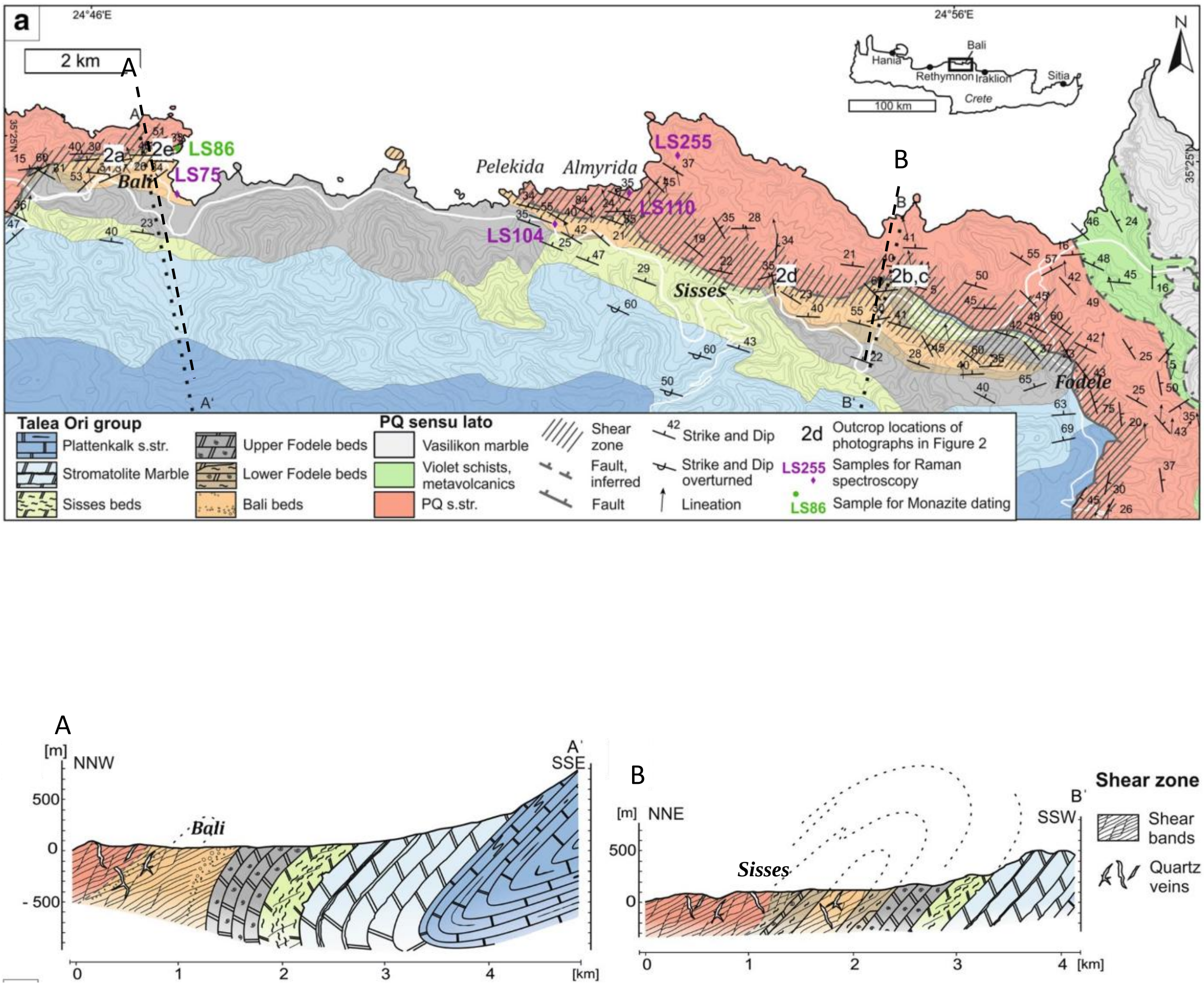

*(**c**) the Talea Ori, central Crete, modified after Epting et al. (1972). The structural data and location of the shear zone are based on Seybold et al. (2019).*

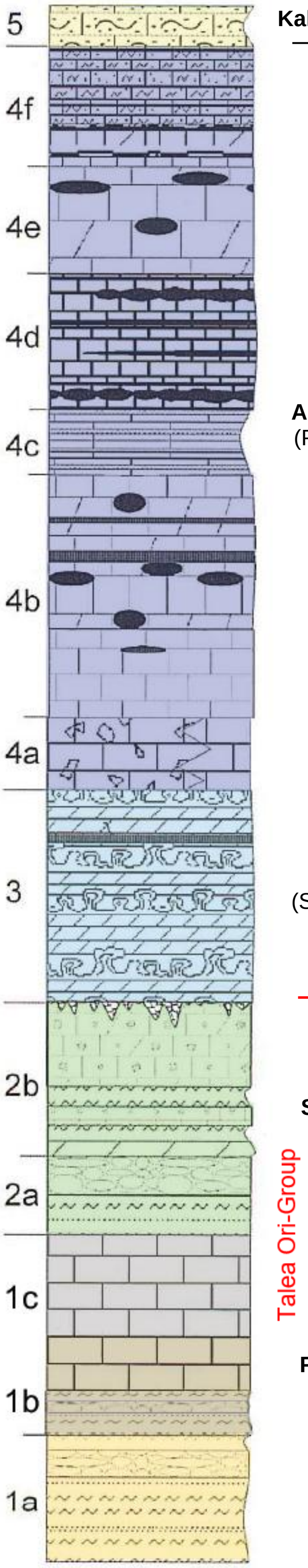

Formation	Description	Age
Kalavros Fm.		**Lower Oligocene**
Aloides Fm. (Plattenkalk)	Calc-phyllite and phyllite f: Thin bedded marble with red and green carbonate silt horizons and sponge remains e: Dark thick marble beds and white chert nodules d: Dark thin marble beds and interlayered white ropy chert layers (silica sponges) c: **"Gingilos-Beds"** Chert-claystone-carbonate sequence (phyllites and yellowish metasandstones) b: Dolomite marbles with chert nodules a: Carbonate breccias and white marbles, dolomitic breccias, stromatolite dolomite marbles	**Liassic – Eocene** Talea Ori: Cephalopods, Kuss, 1982 Krahl et al. 1988. Eastern Crete: Eocene foraminifers, Fytrolakis, 1972; rudists Wachendorf et al. 1980
Mavri Fm. (Stromatolith -Dolomit)	Dolomite or calcite marbles with stromatolites. Transgressional conglomerate at base	**Norian – Liassic** (Foraminifers, Epting et al. 1972)
Sisses Fm.	b: Upper Sisses Fm.: light dolomite marbles partly sericitic, oolite and oncolite marbles. Metabauxite in karst on top a: Lower Sisses Fm.: greenish to violet phyllites, carbonate meta-conglomerate, sericite quartzite	**Lower Triassic - Upper Triassic** a: conglomerate: Upper Triassic: miliolid Foraminifers Kock, 2007; Olenekian: conodonts König and Kuss 1980; Radiometric dating (Seybold et al., 2019)
Fodele Fm.	**c: Upper Fodele Fm**. dark fossil-rich dolomite marble	**Middle to Upper Permian** Corals, fusulinids, bryozoa (Epting et al., 1972)
	b: Lower Fodele Fm. dark dolomite marble, black shales and metasandstones	**Upper Carboniferous - Lower Permian** Brachiopods, trilobites, etc. (König and Kuss 1980) Radiometric dating (Seybold et al., 2019)
	a: Bali and Galinos Beds black schists and phyllites, quartzites, meta-conglomerate, meta-chert, rare patch reef	

Stratigraphy of the Platy Marble Unit (Plattenkalk s.l.) in Central Crete after Manutsoglu et al. 2003, modified after Seybold et al, 2019

2 Bali and South of Mt. Zaphorokipos - Petrol Station

2.1 Lower Fodele Formation - Bali and Galinos Beds

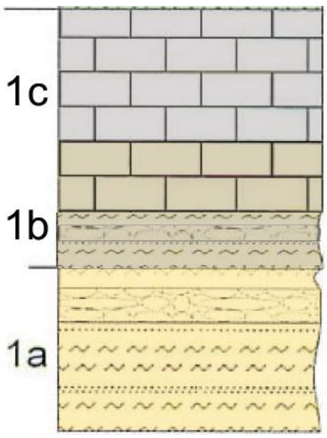	Dark fossil rich marble Dark marble, Black shales Metasandstones, calcic meta-conglomerate **Bali and Galinos Beds** Meta-conglomerate Black phyllites, quartzites, meta-chert, patch reef

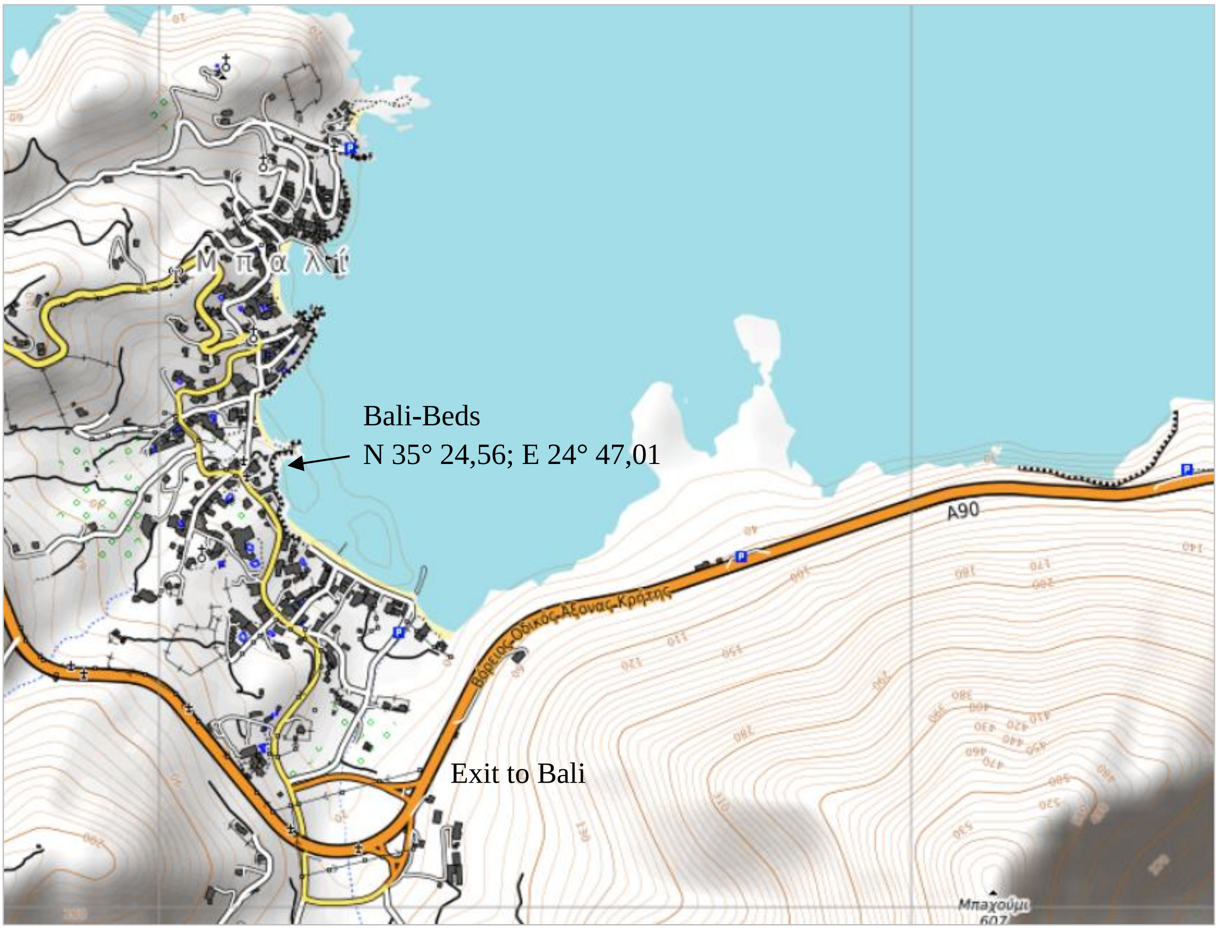

Location of Bali Beds

The Bali-Beds (or Galinos Beds) consist predominantly of siliciclastic sediments that reflect a gradual deepening of marine facies with turbidite features *[Seybold, 2019]*. Zircons from the meta-sandstones found within the Bali beds have been dated by Kock et al, 2007 and Seybold L., et. al., 2019 indicating largely Upper Carboniferous and partly early Proterozoic ages.

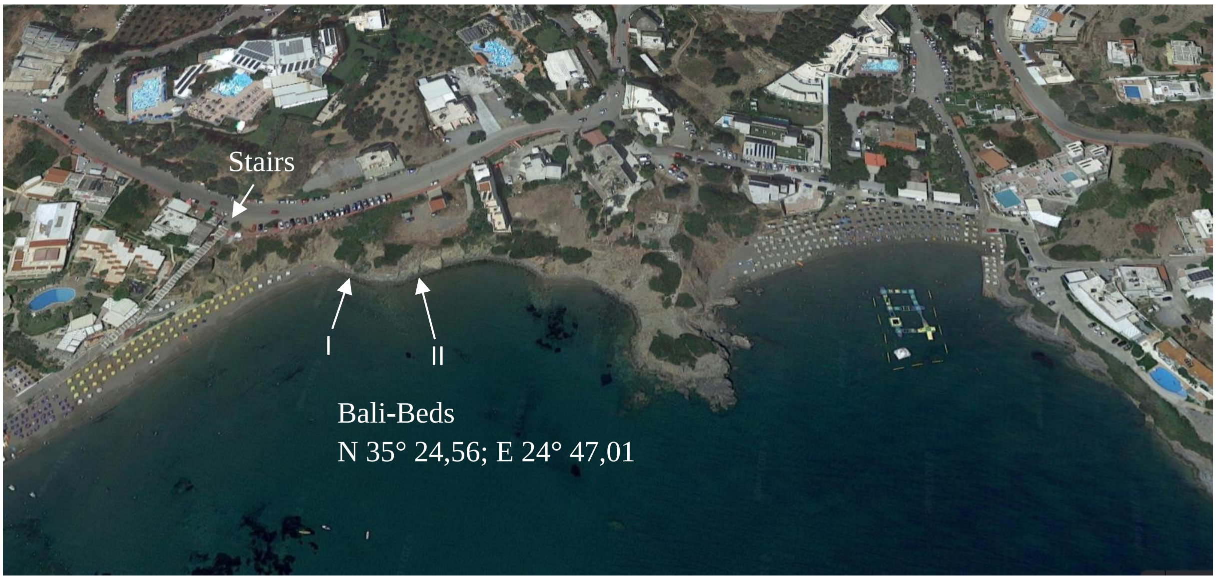

Outcrops at Bail Beach (arrow) [Source of image Google Maps]

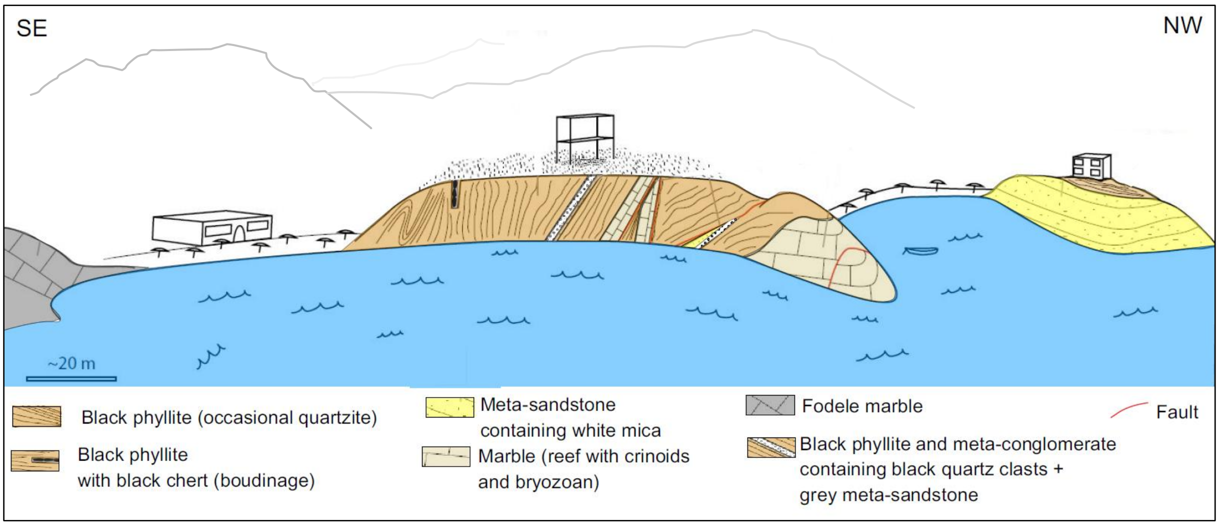

Base of the Talea Ori Group (Bali / Galinos Beds) after Kock (2003) [Stampfli, 2010]

The Bali beds are exposed on the beach immediately next to the village. The formation consists of a series of black shales (also named Galinos shale), metasandstones, meta-conglomerates, black quartzites, black meta-chert (lydite) and locally fossil-rich marbles. The metasandstones are dark greywackes (quartz arenites) that are rich in organic material (graphite) and contain light mica. The black shales have revealed bryozoans, sea urchins and crinoids that indicate sedimentation during the Carboniferous. The black shales are interlaced with conglomerate beds containing predominantly dark quartz, but also other clasts, which implies supply from a wider region (Trepmann et al. 2010). Seybold, 2019 interprets the meta-conglomerates, metasandstones and shales as a turbiditic sequence, owing to the graded bedding, which is inverse at this location due to folding.

Outcrop I: View of the Bali-Beds exposed at the Bali Beach. Sandstone in the foreground and Talea Ori mountains in the background

Outcrop II, Galinos Beds at Bali Beach. 1: Succession of meta-conglomerate; 2: black shale

Outcrop II: Meta-conglomerate boulder containing predominantly black quartz pebbles.

Outcrop II, Meta-conglomerate at Bali Beach. 1: Black quartz clasts. 2: Clasts of other lithologies. Based on the susceptibility to weathering and the roundness of the clasts geologist are able to gain some idea of the distance of transport. In this case the clasts in the sample are both proximal and distal.

Outcrop I, boulder at Bali beach. Conglomerate and sandstone layers indicate deposition of two different turbidity currents.

Outcrop II: Sample of black shale. In weathered condition it turns brown to beige. The marine shale indicates deep water conditions and could represent the background sedimentation in a turbidite sequence.

Outcrop I: Grey metasandstone at Bali Beach

Outcrop I, closeup of previous picture showing metamorphic greywacke. Greywacke is typically found in turbidites and features besides quartz, poorly weathered material such as feldspar and lithic components.

Thin sections show that the feldspar as well as the mica in the meta-sandstones and meta-conglomerates are not only of detrital nature, but are also metamorphic. Aligned porphyroblasts of white mica, biotite, quartz, graphite and rutile form an internal foliation (Seybold et al. 2019). Microscopic analysis also reveals that the meta-chert contains radiolarians and ostracods.

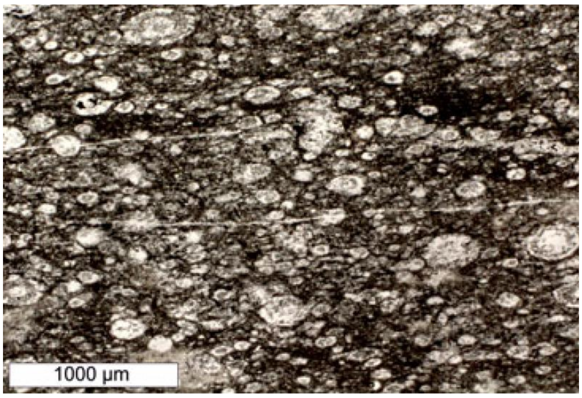

Meta-chert with fossil relics (Bali beach). [Seybold et al. 2019]

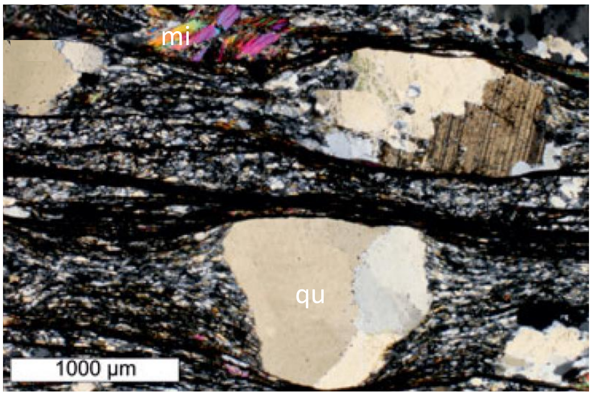

Coarse-grained metasandstone sampled for U–Pb dating of detrital zircons (NW of Bali) (photomicrograph taken with crossed polarizers). qu: Quartz, mi: mica [Seybold et al. 2019]

Kock et al. conducted investigations into the biostratigraphy, sedimentology and zircon provenances of the Talea Ori in 2006. Zircon provenances were determined using Uranium-Lead Isotope Dating. The results show that the Talea Ori mountains and other lateral equivalents in the Hellenides can be attributed to the western continuation of the Cimmerian terrane. The Cimmerian terrane was a long thin land mass that broke off from Pangea during the formation of the Neotethys. It separated the Neotethys in the south from the Palaeotethys in the north from the Late Permian onwards. The opening of the Neotethys is documented by the accumulation of detrital sediments such as conglomerates and sandstones (Bali-Beds) within a rift graben. Detrital zircons ages[1] indicate that during the Late Carboniferous, a river network was flowing from southern Spain/ Calabria and from northwestern Africa towards the Neotethys graben. Deepening of marine conditions due to widening of the rift is indicated by the black shale within the Bali Beds. *[Kock et al, 2007]*

[1] *Note that a sedimentary rock cannot be older than the source of the components it contains. Dating must therefore be regarded as a maximum age, while the true age of sedimentation is likely to be slightly younger.*

2.2 Upper Fodele Formation - South of Mt. Zaphorokipos

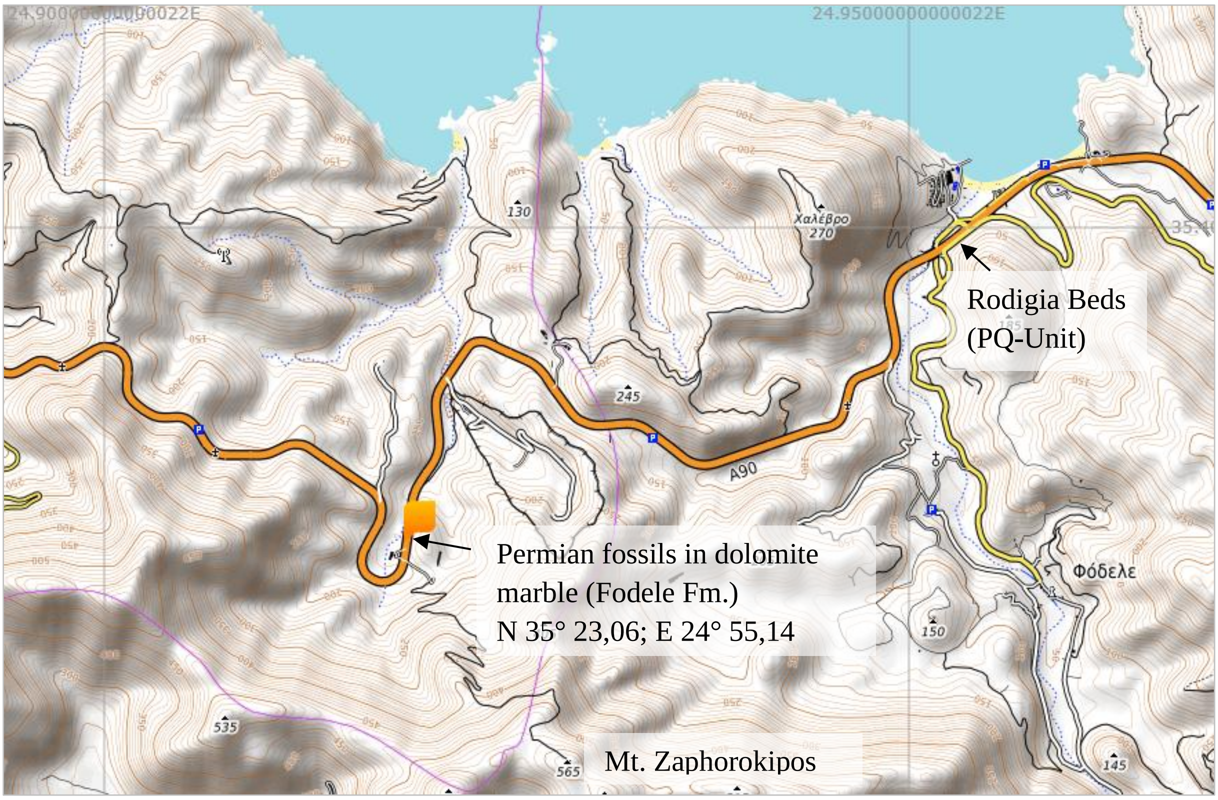

Fodele Fm. of the Talea Ori Group

Outcrops I to IV within the Upper Fodele formation containing Permian fossils [Source of image: Google Maps]

The upper part of the Fodele Formation is exposed on the eastern side of the main road opposite the petrol station, near the hairpin bend. The dark marble contains Permian fossils, which despite the high-pressure metamorphism are well preserved. The outcrop is reported to exhibit corals (*Wentzelella*, *Wentzelophyllum*, *Waagenophyllum*, *Pseudohuangia*), bryozoans (*Fenestella*), brachiopods, bivalves and gastropods (*Bellerophonids*), parts of crinoid stalks, and calcareous algae. They represent a shallow carbonate shelf facies during Permian time.

Outcrop I: Permian fossils in dark marble of the Upper Fodele Fm. Arrow: Coral

Outcrop I: Closeup of previous picture showing coral and possibly brachiopod or bivalve shells next to it.

Outcrop I: Permian fossils within the Upper Fodele Fm. The arrow indicates a "geological spirit level" - the bivalve/brachiopod is upside down as the white calcite filling should be on top, and the dark sediment filling at the bottom. The fossils are very well preserved in spite of HP/LT metamorphism.

The dark Fodele Marbles are interpreted to have once formed a carbonate shelf at the northern margin of the Neotethys in late Permian times.

Some of the bivalves and brachiopod shells are a type of "geological spirit level". The cavities of the fossil shells were only partially filled with sediment during sedimentation, while the remaining space was filled with calcite crystals during diagenesis. At this outcrop the white calcite filling (that should be facing upwards) faces downwards indicating an inverse orientation of the rock. This fits in well with the tectonic concept previously mentioned involving a recumbent anticline limb.

Unfortunately, the outcrop has been covered with a safety net against rock fall since my last visit so that it no longer can be investigated properly.

Outcrop II: Permian fossils possibly bivalves within the Upper Fodele Fm.

Outcrop III: Permian crinoids within the Upper Fodele Fm. Boxes show enlargement (see following pictures)

Outcrop III, A: 1: Weathered marble surface displaying individual crinoid stem pieces (columnals), 2: possible brachiopod shell


Outcrop III, B: 1: Individual crinoid stem pieces (columnals)

Outcrop IV: Overview of outcrop, Upper Fodele Fm.

Outcrop IV: Individual crinoid stem remains and possibly brachiopod as well as bivalve shells

Outcrop IV: Closeup displaying crinoid stem fragments and possibly brachiopod as well as bivalve shells

3 Sisses – Aloides Traverse

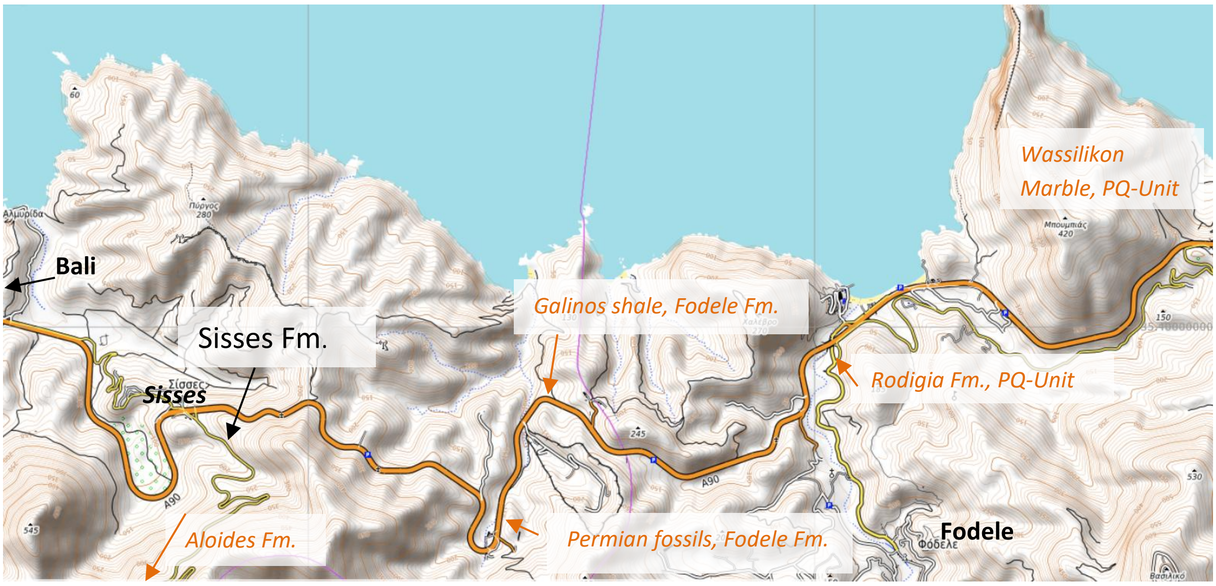

Overview of the area around the Sisses village showing the location of the Sisses Formation

Overview of the Talea Ori Mts. looking East [Source of image: Google Maps]

Overview of the lower part of the Sisses-Aloides Travers looking south. At this location the rock lies in an inverse position so that the various formations may be examined from the base upwards. [Source of image: Google Maps]

3.1 Fodele Formation

Fodele Fm. Picture taken next to the main road underpass

Near the village of Sisses the Fodele Formation is exposed at the road cuts along the main Northern Highway and near the underpass. The Fodele Beds consist of dark dolomitic marbles, which date back to the Permian approximately 300 million years ago (see also previous Section “Dolomite Marbles with Permian Fossils”). A few tens of meters towards the north the section passes into the white marbles of the “Sisses beds” that are approximately 280 million years old.

3.2 Sisses Formation

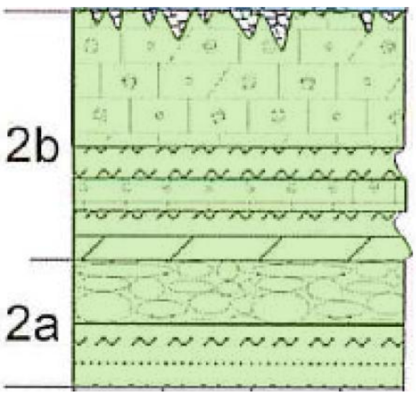

2b	Upper Sisses Beds Meta-bauxite in karst Oolite and oncolite marbles. -Oncolite marbles -Light dolomite marbles, partly sericitic
2a	Lower Sisses Beds - Carbonate meta-conglomerate, - Greenish and violet phyllites Sericite quartzite

The Fodele Formation is concordantly overlain by the Sisses Formation that consists mainly of white marble beds. Due to local erosion during mountain building, significant thickness variations are recorded in the Sisses formation throughout the Talea Ori unit *[S. Kock, 2007]*.

3.2.1 Carbonate Meta-Conglomerate

Sample from the main road east of Sisses. Meta-conglomerate from the Sissies Fm. with carbonate clasts up to 5 cm in diameter displaying strain caps (1) and shadows (2). The carbonate clasts contain various relic recrystallized fossils [Seybold et al., 2019].

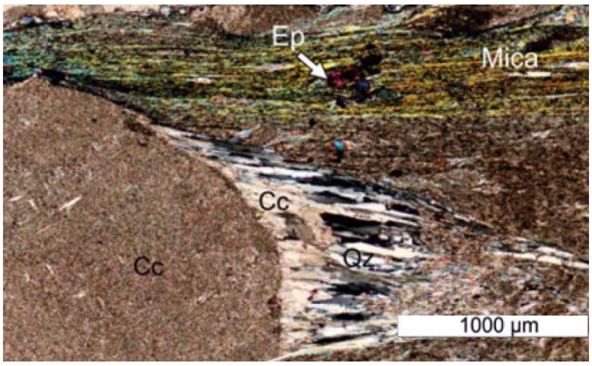

Carbonate clasts form complex strain shadows composed of calcite (Cc), quartz (Qz) and mica. Epidote and albite blasts have inclusions forming internal fabrics. [Seybold et al., 2019].

3.2.2 Pink Marble and Phyllite/Schist

Locally greenish and reddish phyllites and quartzites appear in the sequence. The upper part of the Sisses Formation reveals light, sometimes slightly pink coloured, calcitic and dolomitic marbles containing oncoids and ooids. They originated from shallow-water limestones and were transformed into marble by HP/LT metamorphism. Olenecian conodonts have been found in the lower Sisses beds (König and Kuss, 1980) *[Kull]*. Within the Sisses beds there is also a layer of calcic conglomerate the clasts of which contain foraminifers. The conglomerate contains clasts featuring Fodele limestone and micritic limestone containing a miliolid foraminifer species. The discovery of the foraminifers in some of the clasts enabled Koch et. al. 2007 to assign a Late Triassic age to the conglomerate, thus requiring the overlying phyllites and oolitic limestone to be younger or of similar age *[S. Kock, 2007]*.

The Sisses formation extends as far as the first sharp hairpin bend and ends there with an erosional unconformity which is overlain by the Mavri Formation.

I: Disused quarry (now a field) 1: Sisses marble 2: Phyllites and schist.

I: Red and grey coloured phyllite/schist formed by HP/LT metamorphism. Talus at the foot of the cliff

I: Marble with sericite. Talus at foot of the cliff. 1: fine layer of sericite, 2: marble

I: Sisses Fm.; pink coloured marble

I: Closeup of previous picture: Pink coloured marble

3.2.3 Oncoids

I: Sisses Fm. Oncoids are layered structures formed by cyanobacterial growth. They are very similar to stromatolites, but instead of forming columns, they form spherical type structures usually around an existing nucleus. Oncolites are indicators of warm waters in the photic zone.

Sericite is the name given to very fine, ragged grains and aggregates of white (colourless) micas, typically made of muscovite, illite, or paragonite. Sericite occurs as the fine mica that gives the sheen to phyllite and schistose metamorphic rocks. It is also produced by the alteration of orthoclase or plagioclase feldspars in areas that have been subjected to hydrothermal alteration.

3.2.4 Oolite

Overview of the outcrop II: Sisses Fm. 1: Oolite bed


II: Closeup of previous picture.

II: Closeup of previous picture. The ooids are quite small approx. 0.5mm - 1mm in diameter. Dolomitic ooids are most likely the result of the replacement of the original texture in limestone.

Hand sample of Sisses marble from near the transition to the Mavri Formation. 1: The marble is very light and contains some ooids. 2: Small intraclast

Ooids are usually formed in warm, supersaturated, shallow, highly agitated marine intertidal environments. The mechanism of formation starts with a small fragment of sediment acting as a 'seed', such as a piece of a shell. Strong intertidal currents wash the 'seeds' around on the seabed, where they accumulate layers of chemically precipitated calcite from the supersaturated water. The size of the oolites reflect the time that they were exposed to the water before they were covered with later sediment.

3.3 Sisses Formation - Palaokarst with Lateritic Fillings

See My GeoGuide No. 28: The Plattenkalk Unit in the Talea Ori Mountains, Vossakos Traverse

4 Mavri Formation

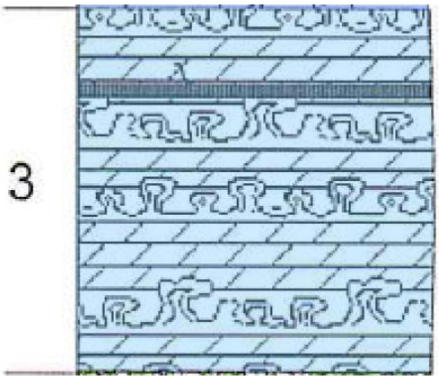	Dolomite marbles with stromatolites

Outcrop III, Mavri-Fm. Stromatolith Dolomit in an inverted position

The Mavri Formation was formed during the Rhaetian to lower Jurassic. At the base of the Mavri Formation a transgression conglomerate can be found in several places. The conglomerate contains clasts from the Sisses Beds (oolitic limestone), the Fodele Beds and clasts of stromatolite dolomite. The matrix contains Norian and Rhaetian foraminifera. The hiatus between the Sisses Formation and the Mavri Formation is reported to have been only for a short time.

Outcrop III, Mavri-Fm. Stromatolith Dolomit in an inverted position (see Appendix)

Outcrop III, Mavri-Fm. Hand sample from the Mavri-Fm, displaying dark stripes either from organic material or from stromatolites.

The Mavri Formation is a very thick, homogeneous, dolomite sequence consisting of light to dark grey striped marble and dolomites. The banding is caused by varying amounts of organic substances, and iron-rich layers also occur. The stromatolite dolomite gets its name from the frequent occurrence of stromatolites that leave dark wavy patterns within the marble. The stromatolites are evidence of very shallow water conditions (see Appendix).

Outcrop III, Mavri-Fm. 1: Intraclasts indicating high energy conditions e.g. a storm or tectonic movement. 2: "Bird's eye"

Intraformational breccias and bird's eyes structures can be observed in many places within the Mavri Formation [*Kock et al, 2007]*. Intraformational conglomerates and breccias contain clasts that derive from the same sedimentary formation which they are part of. The clasts have the same or similar composition as the matrix that surround them. These rocks are produced by events of brecciation or clastic reworking that interrupt the normal sedimentation of a basin, for example a storm or an episode of emersion. Such events produce intraformational limestone clasts such as rip-up clasts torn off the bottom of a basin by a current.

Outcrop IV, Mavri-Fm. Stromatolith Dolomit

Outcrop IV, Mavri-Fm. Stromatolith Dolomite

Outcrop IV, Mavri-Fm. Stromatolith Dolomite

Outcrop V, massive white dolomite marble could be the transition to the Aloides Fm.

Outcrop V, hand sample of massive white dolomite marble displaying numerous cavities

5 Aloides Formation (Plattenkalk)

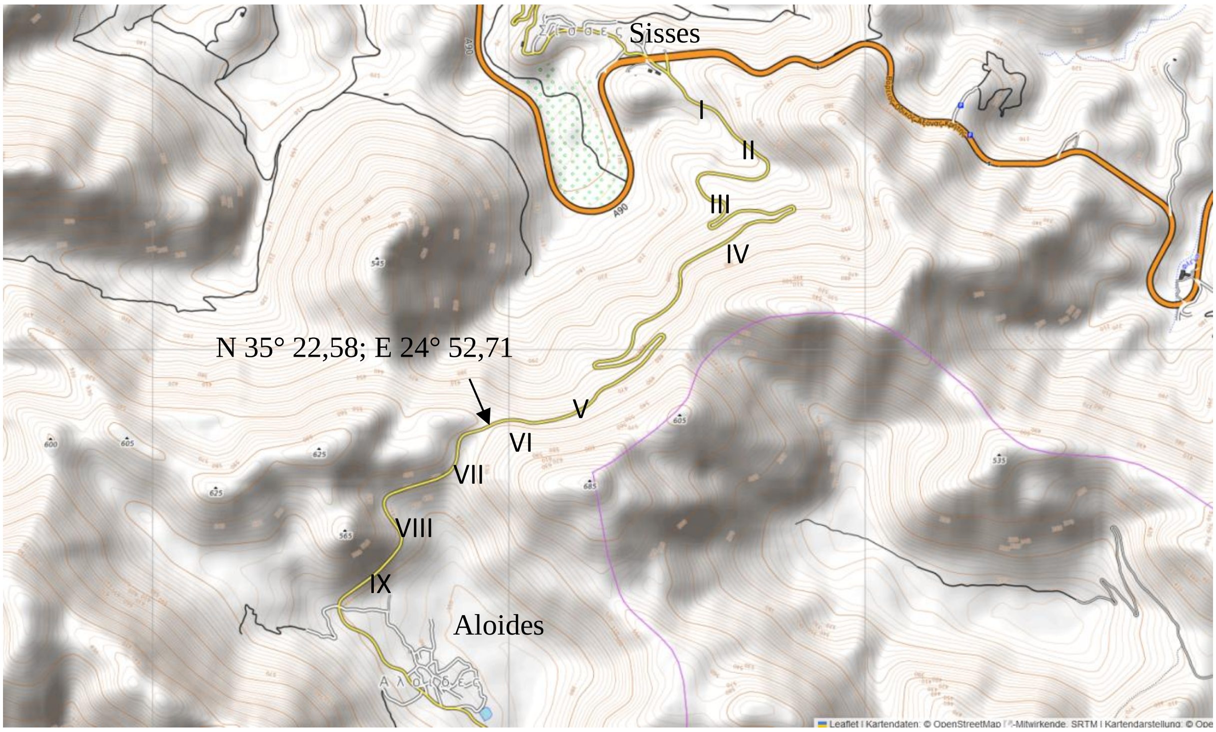

Location of outcrops. Arrow indicates the base of Aloides Formation at the mountain pass leading to the village of Aloides

Locations of outcrops, Aloides Formation [Source of image Google Maps]

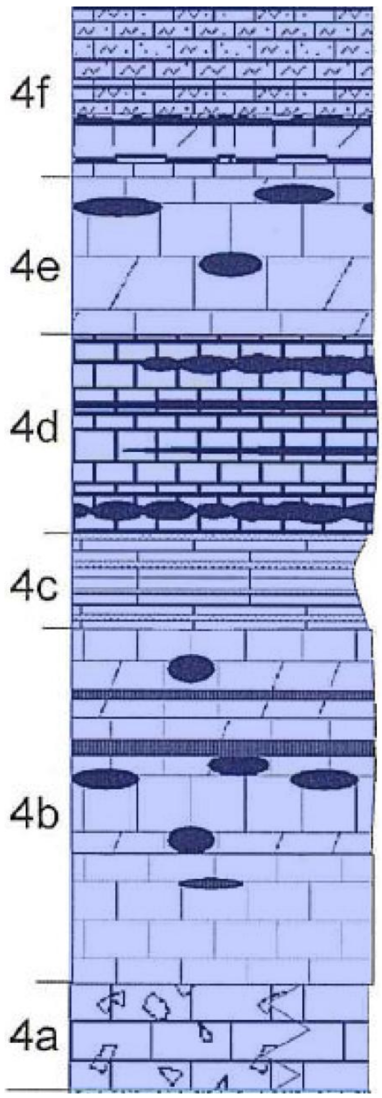

Thin bedded marble with red and green carbonate silt horizons and sponge remains
Middle to thick bedded calcitic marbles, white chert-nodules and -layers
Dark thin calcitic marble beds and interlayered white ropy chert layers (possibly silica sponges)
Gigilos-Beds: Chert-claystone-carbonate sequence (phyllites and yellowish metasandstones)
Dolomite marbles with white chert nodules and layers
Dark platy marble with white chert nodules
Platy marble
Carbonate and dolomitic breccias passing into white marbles, stromatolite dolomite marbles

Section of the Aloides Formation at the Talea Ori Mountains, Central Crete [Manutsoglu et al. 2003]

The Aloides formation begins at the pass at the mountain ridge. The typical features of the Platy Marble can be observed along the road that leads to the village of Aloides. The Plattenkalk or Aloides Formation forms a monotonous sequence of thick-banked, often coarsely recrystallised, and thin-banked, finely crystalline grey limestone marbles with numerous chert layers and chert nodules.

5.1 4a- Carbonate and Dolomitic Breccias

The transition from the Mavri Formation to the Aloides Formation differs from the rest of the formation as it consists of massive, barely banked marbles and dolomite marbles with little or no chert nodules. Manutsoglu et al. 2003 describes the basal beds as carbonate and dolomitic breccias passing into white marbles.

Outcrop VI (4a), light grey marble breccia at the pass to the next valley

Outcrop VI (4a), closeup of previous picture. Marble breccia containing silica 1: Trace of steel from nail indicating silica content, 2: Clast

Outcrop VI (4a), light grey marble breccia

5.2 4b - Dark Platy Marble with White Chert Nodules

Outcrop VII (lower part of 4b). Dark platy marble with no or hardly any chert nodules.

Up section where a succession of dark grey platy marbles begins intercalated marble beds containing bitumen have been reported *[Kull]*.

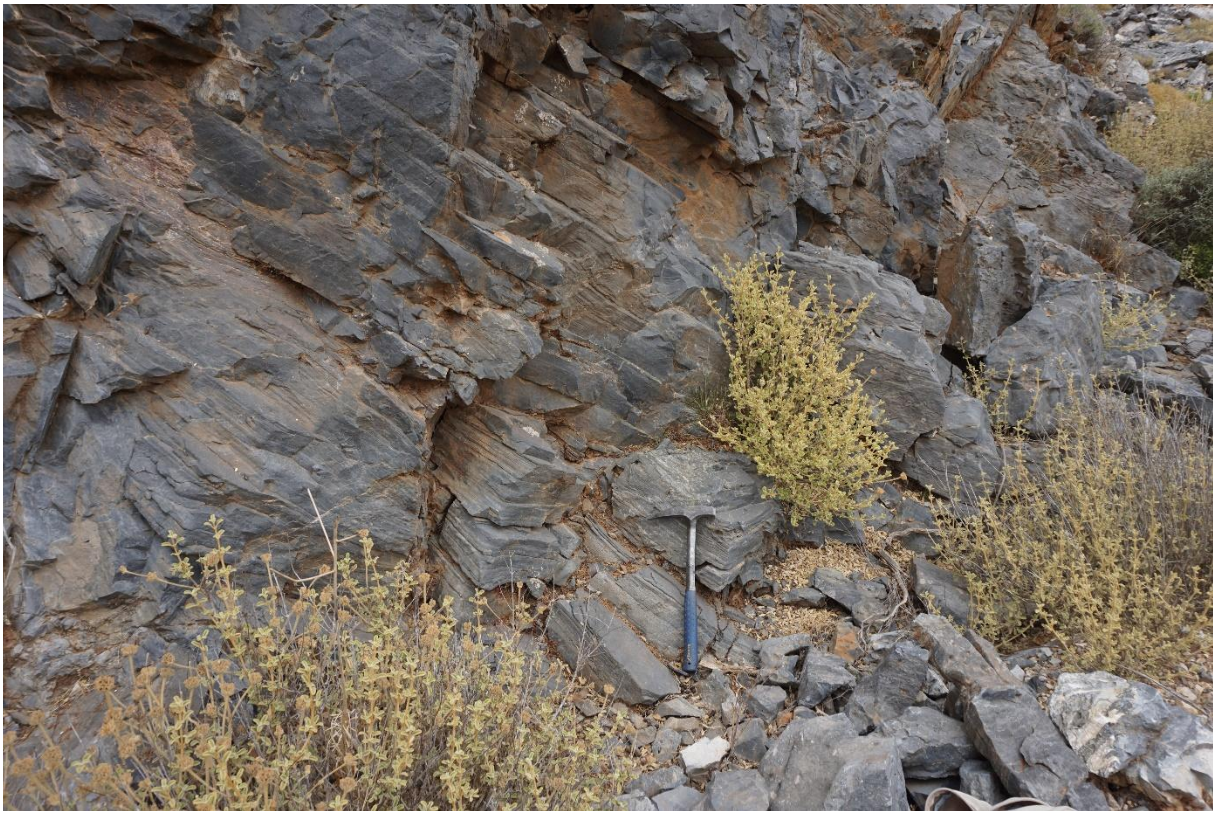

Outcrop VII (lower part of 4b), Closeup of previous picture. The stripy pattern parallel to the bedding may be partly due to stromatolites.

Outcrop VII (lower part of 4b), Marble breccia.

5.3 4d - Dark Thin Calcitic Marble with Ropy Chert Nodules and Chert Layers

Outcrop IX (4d), dark marble with chert nodules and layers 1: dark thin beds of marble, 2: white chert nodule probably a former sponge. 3: Chert debis.

Outcrop IX (4d), chert nodules with rings embedded within the platy marble beds. The chert concretions cross cut the fine stratification and were therefore formed late diagenetically. Occasionally the nodules display rings. [Kull]

6 Plate Tectonics:

During the Upper Carboniferous to the Triassic, the sedimentation of the Platy Marble Unit (Plattenkalk) took place at the western continuation of the Cimmerian block. This was a shelf area of a microplate located at the northern edge of the emerging Neotethys Ocean (i.e. today's eastern Mediterranean). The sedimentation area of the Phyllite-Quartzite unit lay to the north in the Palaeotethys area (see following figures). *[Kull]*

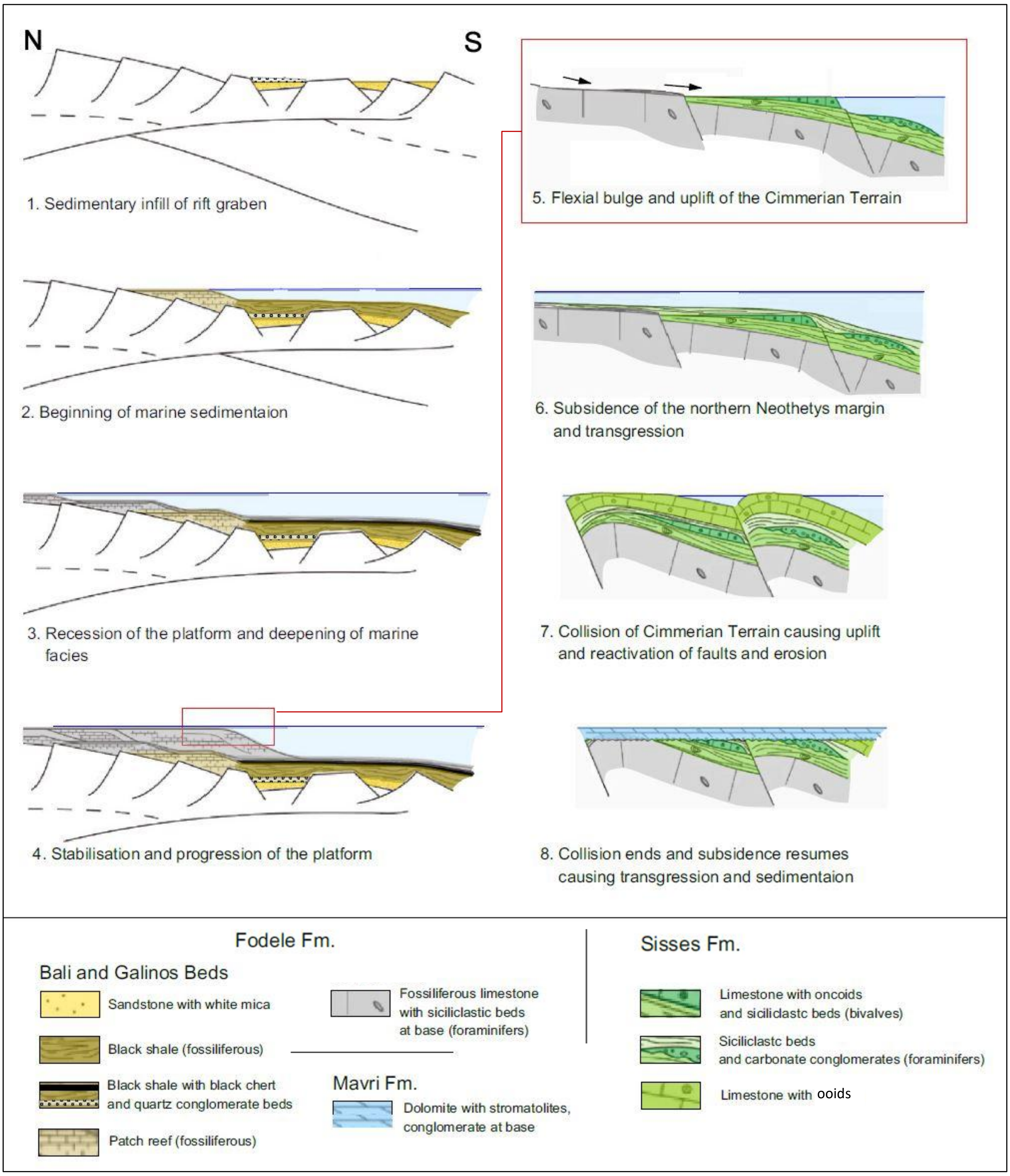

Model showing the development of the Fodele and Sisses formations from rift to carbonate shelf sediments up until the collision of the Cimmerian Terrain [Stampfli, 2010]

Kock S. et al., 2007 conducted investigations into the biostratigraphy, sedimentology and zircon provenances (Uranium-Lead Isotope Dating) of the Talea Ori in 2006. The results showed that the Talea Ori mountains and other lateral equivalents in the Hellenides could be attributed to the western continuation of the Cimmerian terrane, which separated the Neotethys in the south from the Palaeotethys in the north during the Late Permian onwards. The Palaeotethys gradually closed during the Upper Triassic due to subduction at the Eurasian plate margin (Stampfli et al. 2002, Kock et al. 2007). This was expressed in the Talea Ori by a major eo-Cimmerian unconformity at the Sisses-Mavri erosional boundary. Uplift causing a hiatus can be attributed to flexural bulging of the subducting Cimmerian terrane, followed by local tectonic inversion of tilted blocks of the northern Neotethys margin (see figure above). *[Kock et al, 2007]*

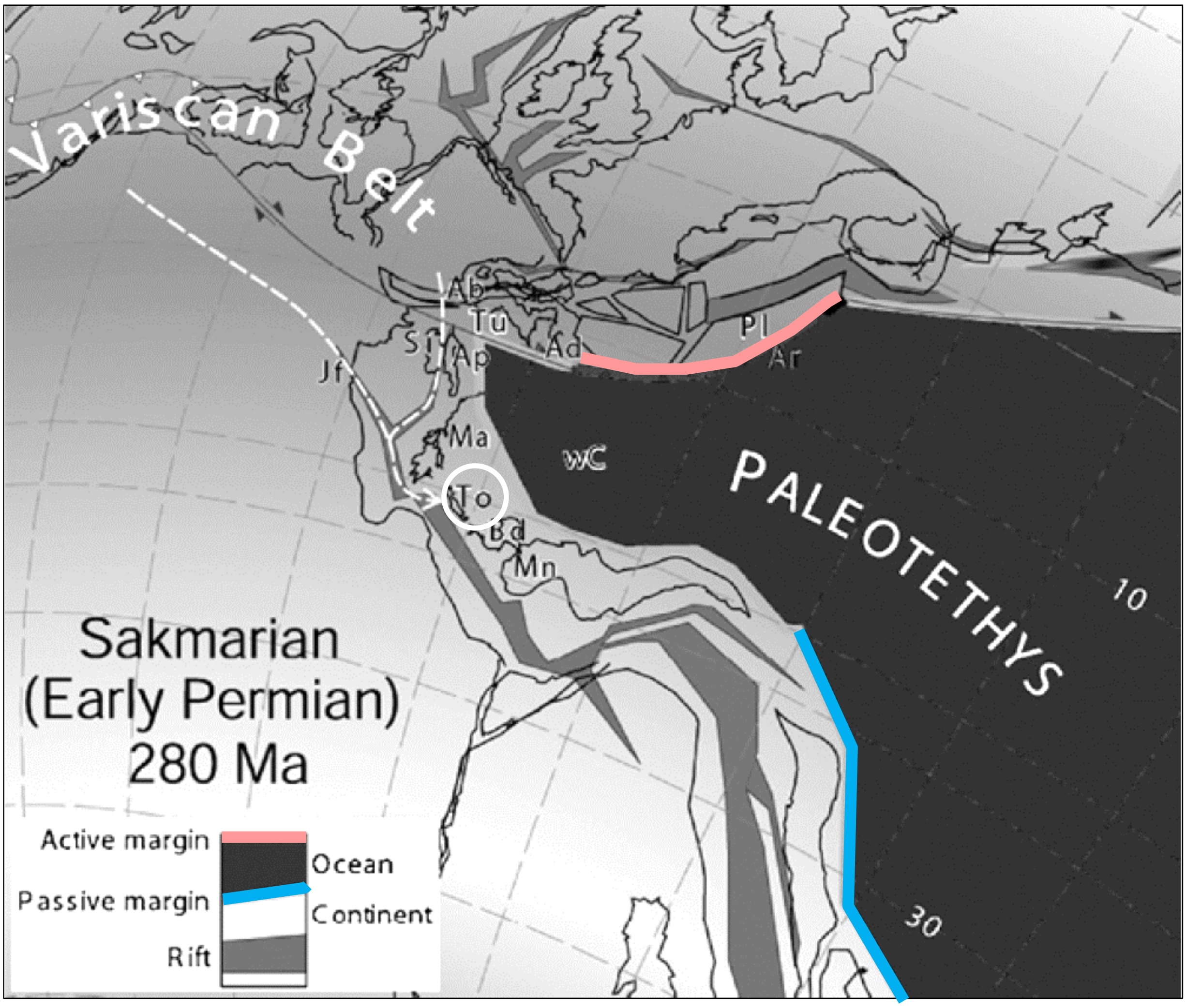

Positions of tectonic plates in the Sakmarian (Early Permian 280 Ma) (after Stampfli and Borel (2002). At this time, the subduction of the Palaeotethys ocean induced extension along its southern margin, thus slowly separating the Cimmerian micro-continent (of which the Talea Ori was a part) from the Gondwanan mainland, with formation of rifts (see also Stampfli et al., 2003, Fig. 8). The arrow shows the assumed provenance and transport routes of the analyzed zircons. Ab: Alboran, Ad: Adria, Ar: Arna, Ap: Apulia, Bd: Beydaghlari, Jf: Jeffara, Ma: Mani, Mn: Menderes, Pl: Pelagonian, Si: Sicily, To: Talea Ori, Tu: Tuscan, wC: Western Crete (Phyllite–Quartzite). [Kock et al. 2007]

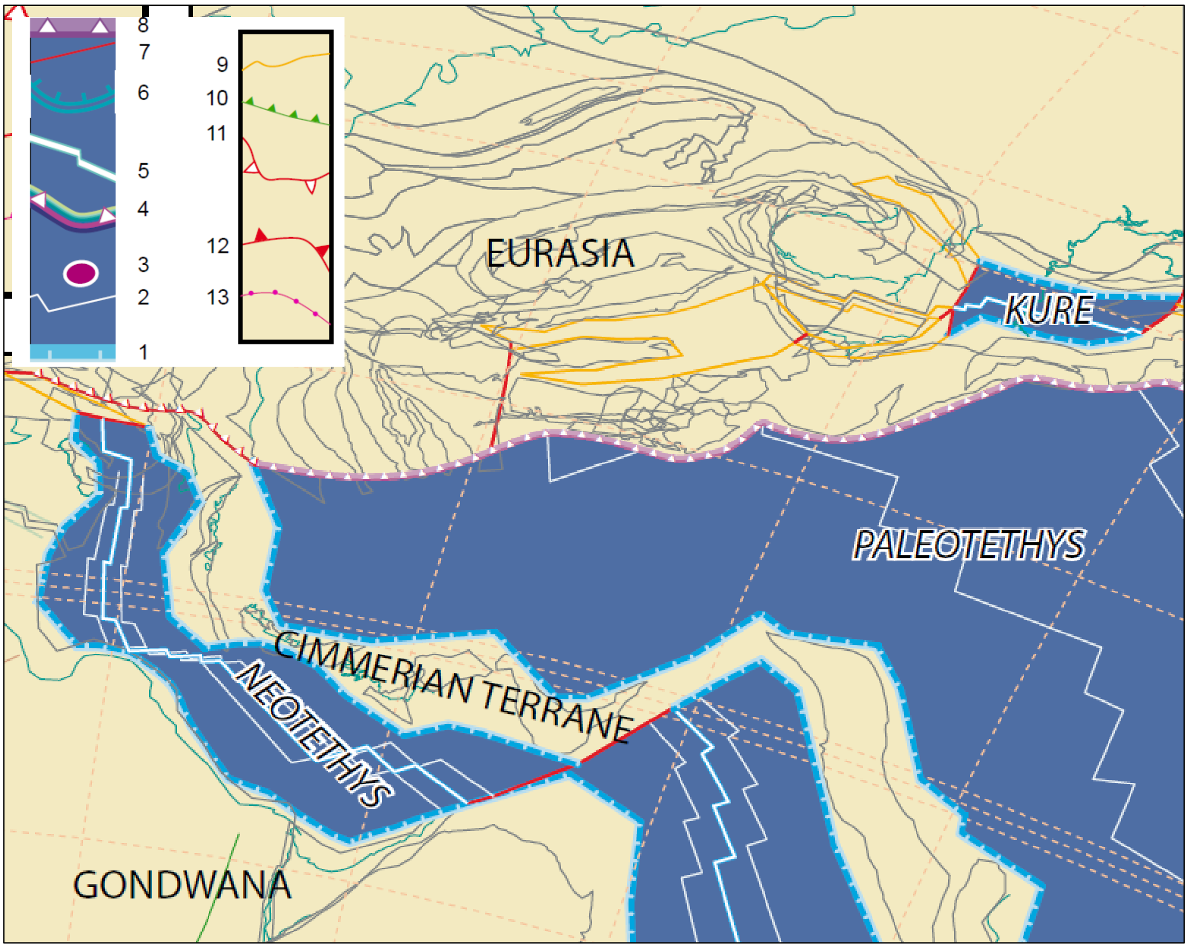

Positions of tectonic plates during the in the Olenekian (250 Ma) after Stampfli. 1. passive margin; 2. magnetic anomalies or synthectic anomalies; 3. seamount; 4. intraoceanic subduction/arc complex; 5. spreading ridges; 6. obductions; 7. Transform and strike-slip faulting; 8. subduction zone; 9. rifts; 10. inversion zones; 11. collision zones; 12. Active thrusts; 13. Sutures.

References

Chatzaras, v., Xypolias, P. & Doutsos, T (2006): Exhumation of high-pressure rocks under continuous compression: a working hypothesis for the southern Hellenides (centralCrete. Greece). - Geol. Mag. 143: 859-R76.

Epting, M., Kudrass, H.-R., Leppig, U. & Schafer, A. (1972): Geologie der Talea Ori/Kreta. - N. Jb. Geol. Palaont. Abh. 141: 259-285.

Fassoulas C., Rahl J.M., 2004: Patterns and Conditions of Deformation in the Plattenkalk Nappe, Crete, Greece: A Preliminary Study, Natural History Museum of Crete, Yale University, New Haven, Connecticut

Hall, R. &Audley-Charles. M.G. (1983): The structure and regional significance of the Talea, Ori, Crete. - J. Struct. Geol. 5: 167-179.

Kull U., 2012: Kreta, Sammlung geologischer Führer

Kock S. et al, 2007: Detrital zircon and micropalaeontological ages as new constraints for the lowermost tectonic unit (Talea Ori unit) of Crete, Greece, Geologisch-Paläontologisches Institut der Universität Basel

Krahl, J., Richter, D., Forster, 0., Kozur, H. & Hall, R. (1988): Zur Stellung der Talea Ori im Bau des kretischen Deckenstapels (Griechenland). - Z. dtsch. geol. Ges. 139: 191-227.

Manutsoglu, E., Soujon, A., Reitner, J. & Dornsiepen, U.F. (1995a): Relikte lithistider Demospongiae aus der metamorphen Plattenkalk-Serie der Insel Kreta (Griechenland) und ihre palaobathymetrische Bedeutung. - N. Jb. Geol. Palaont. Mh. 1995: 235-247.

Rahl J. M., Fassoulas C., Brandon M. T., 2004: Exhumation of high-pressure metamorphic rocks within an active convergent margin, Crete, Greece: Field Trip Guide Book - B32 32nd International Geological Congress, Department of Geology and Geophysics, Yale, University, New Haven, Connecticut 06511, U.S.A., Natural History Museum of Crete, University of Crete, Heraklion 71409, Greece

Seybold L., 2019: New constraints from U–Pb dating of detrital zircons on the palaeogeographic origin of metasediments in the Talea Ori, central Crete, Ludwig-Maximilians-Universität, Luisenstraße 37, 80333 Munich, Germany

Stampfli 2010: Stampfli Field Course, Tectonostratigraphy and Plate Tectonics of Crete, Université de Lausanne, France

Theye, T, Seidel, E. & Vidal, O. (1992): Carpholite, sudoite and chloritoid in low-grade high-pressure metapelites from Crete and the Peloponnese, Greece. - Europ, J. Mineral.
4 487-507.

Thomson, S.N., Stockhert, B. & Brix, M.R. (1998a): Thennochronology of the high-pressure metamorphic rocks of Crete, Greece: implications for the speed of tectonic processes. - Geology 26: 259-262.

Trepmann, e., Lenze, A. & Stockhert, B. (2010): Static recrystallization of vein quartz pebbles in a high-pressure-low-temperature metamorphic conglomerate. - 1. Struct. Geol. 32: 202-215.

Zulauf G. et al., 2014: Closure of the Paleotethys in the External Hellenides: Constraints from U–Pb ages of magmatic and detrital zircons (Crete), Goethe University, Frankfurt a.M., Germany, University of Patras, GR-26500, Patras, Greece

7 Appendix

Geological Time Scale

Eonothem/Eon	Erathem/Era	System/Period	Series/Epoch	Stage/Age	mya[1]
Phanerozoic	Cenozoic	Neogene			2.58
			Pliocene	Piacenzian	3.600
				Zanclean	5.333
			Miocene	Messinian	7.246
				Tortonian	11.63
				Serravallian	13.82
				Langhian	15.97
				Burdigalian	20.44
				Aquitanian	23.03
		Paleogene	Oligocene	Chattian	27.82
				Rupelian	33.9
			Eocene	Priabonian	37.8
				Bartonian	41.2
				Lutetian	47.8
				Ypresian	56.0
			Paleocene	Thanetian	59.2
				Selandian	61.6
				Danian	66.0
	Mesozoic	Cretaceous	Upper	Maastrichtian	72.1 ± 0.2
				Campanian	83.6 ± 0.2
				Santonian	86.3 ± 0.5
				Coniacian	89.8 ± 0.3
				Turonian	93.9
				Cenomanian	100.5
			Lower	Albian	~113
				Aptian	~125.0
				Barremian	~129.4
				Hauterivian	~132.9
				Valanginian	~139.8
				Berriasian	~145.0

Eonothem/Eon	Erathem/Era	System/Period	Series/Epoch		Stage/Age	mya[1]
Phanerozoic	Mesozoic	Jurassic				~145.0
			Upper		Tithonian	152.1 ± 0.9
					Kimmeridgian	157.3 ± 1.0
					Oxfordian	163.5 ± 1.0
			Middle		Callovian	166.1 ± 1.2
					Bathonian	168.3 ± 1.3
					Bajocian	170.3 ± 1.4
					Aalenian	174.1 ± 1.0
			Lower		Toarcian	182.7 ± 0.7
					Pliensbachian	190.8 ± 1.0
					Sinemurian	199.3 ± 0.3
					Hettangian	201.3 ± 0.2
		Triassic	Upper		Rhaetian	~208.5
					Norian	~227.0
					Carnian	~237.0
			Middle		Ladinian	~242.0
					Anisian	247.2
			Lower		Olenekian	251.2
					Induan	251.902 ± 0.024
	Paleozoic	Permian	Lopingian		Changhsingian	254.14 ± 0.7
					Wuchiapingian	259.1 ± 0.5
			Guadalupian		Capitanian	265.1 ± 0.4
					Wordian	268.8 ± 0.5
					Roadian	272.95 ± 0.11
			Cisuralian		Kungurian	283.5 ± 0.6
					Artinskian	290.1 ± 0.26
					Sakmarian	295.0 ± 0.18
					Asselian	298.9 ± 0.15
		Carboniferous	Pennsylvanian[2]	Upper	Gzhelian	303.7 ± 0.1
					Kasimovian	307.0 ± 0.1
				Middle	Moscovian	315.2 ± 0.2
				Lower	Bashkirian	323.2 ± 0.4
			Mississippian[2]	Upper	Serpukhovian	330.9 ± 0.2
				Middle	Visean	346.7 ± 0.4
				Lower	Tournaisian	358.9 ± 0.4

Eonothem/ Eon	Erathem/ Era	System/ Period	Series/ Epoch	Stage/ Age	mya[1]
Phanerozoic	Paleozoic	Devonian	Upper	Famennian	358.9 ± 0.4
				Frasnian	372.2 ± 1.6
			Middle	Givetian	382.7 ± 1.6
				Eifelian	387.7 ± 0.8
			Lower	Emsian	393.3 ± 1.2
				Pragian	407.6 ± 2.6
				Lochkovian	410.8 ± 2.8
		Silurian	Pridoli		419.2 ± 3.2
			Ludlow	Ludfordian	423.0 ± 2.3
				Gorstian	425.6 ± 0.9
			Wenlock	Homerian	427.4 ± 0.5
				Sheinwoodian	430.5 ± 0.7
			Llandovery	Telychian	433.4 ± 0.8
				Aeronian	438.5 ± 1.1
				Rhuddanian	440.8 ± 1.2
		Ordovician	Upper	Hirnantian	443.8 ± 1.5
				Katian	445.2 ± 1.4
				Sandbian	453.0 ± 0.7
			Middle	Darriwilian	458.4 ± 0.9
				Dapingian	467.3 ± 1.1
			Lower	Floian	470.0 ± 1.4
				Tremadocian	477.7 ± 1.4
		Cambrian[3]	Furongian	Stage 10	485.4 ± 1.9
				Jiangshanian	~489.5
				Paibian	~494.0
			Series 3	Guzhangian	~497.0
				Drumian	~500.5
				Stage 5	~504.5
			Series 2	Stage 4	~509.0
				Stage 3	~514.0
			Terreneuvian	Stage 2	~521.0
				Fortunian	~529.0
					541.0 ± 1.0

	Eonothem/ Eon	Erathem/ Era	System/ Period	mya[1]
Precambrian	Proterozoic	Neoproterozoic	Ediacaran	541.0 ± 1.0
			Cryogenian	~635
			Tonian	~720
		Mesoproterozoic	Stenian	1,000
			Ectasian	1,200
			Calymmian	1,400
		Paleoproterozoic	Statherian	1,600
			Orosirian	1,800
			Rhyacian	2,050
			Siderian	2,300
	Archean	Neoarchean		2,500
		Mesoarchean		2,800
		Paleoarchean		3,200
		Eoarchean		3,600
	Hadean[4]			4,000
				~4,600

Geodynamic Model by Stampfli

For numerous years, the group headed by Prof. Stampfli at the university of Lausanne has been working on plates tectonic reconstruction models. The models are constantly evolving due to the addition of new data.

Breakup of Pangea and the Cimmerian Collision

Since the mid Permian (Roadian), the Paleotethys was being subducted northwards under the Eurasia plate. By the Lower Triassic the Cimmerian terrane had already detached itself from the Gondwana northern margin and in doing so initiated the opening of the Neotethys. At the same time Southern Eurasia was strongly subjected to extensional stress due to the roll-back of the Paleothetys oceanic plate during subduction. This caused the opening of a number of back-arc basins starting with the Küre basin in the East. During the Middle Triassic, the Meliata and the Maliac basins opened causing the detachment of the Pelagonian terrane. Owing to the northward subduction of Paleothetys oceanic plate, and the resulting Cimmerian collision at the beginning of Late Triassic, the western part of Neotethys stopped spreading. At the same time, the Pindos back-arc basin opened within the southern Pelagonian margin. Between middle Carnian and early Norian, the Paleotethys was completely subducted and the Cimmerian collision had taken effect on the whole of the western Tethys. The Neotethys started to subduct under the Huğlu back-arc, but when its ocean ridge reached the subduction trench, the subduction was halted and transferred to the North by transform faults, leaving the Huğlu basin open. Further north, the intra-oceanic subduction of the Maliac ocean under the Izmir-Ankara ocean began, which triggered the formation of Vardar supra-subduction-zone (SSZ) since the Rhaetian *[Stampfli, 2010]*.

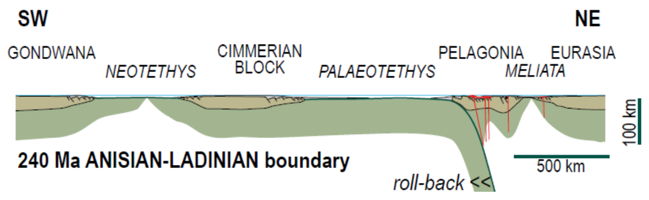

During the Anisian-Ladinian the Paleotethys was subducting northwards against Greater Pelagonia causing lower plate extension, which was offset by spreading of the Neotethys ridge. Additionally, the Paleotethyan slab was rolling back, inducing extension in the upper plate too. The Meliata back-arc basin was already spreading separating the Pelagonian microcontinent from the Eurasian margin, whereas the Maliac basin had just started its synrift stage.

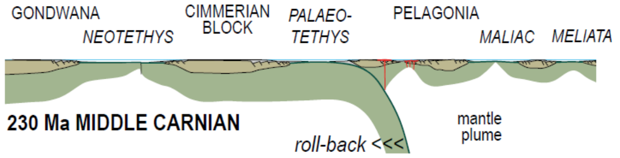

Because of the Cimmerian collision further eastwards of this section (see section line on the following figures) the Neotethys ridge in this region stopped spreading. However, extension is still active in the back-arc realm, where the spreading ridge switched from the Maliac basin to the beginnings of the newly created Pindos basin (see next Figure).

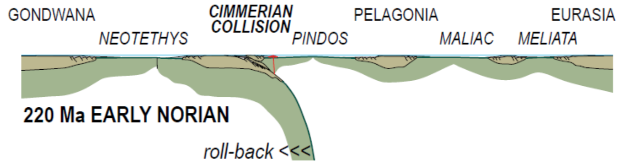

By the early Norian the Paleotethys ocean and its arc was completely consumed and collided with the Cimmerian block causing a phase of mountain building called the Cimmerian collision. The Pindos ridge stopped spreading and sedimentation within the basin becomes pelagic. At about 210Ma, the Paleotethyan

	subducted slab detaches and the Pindos basin started to subside as a whole.
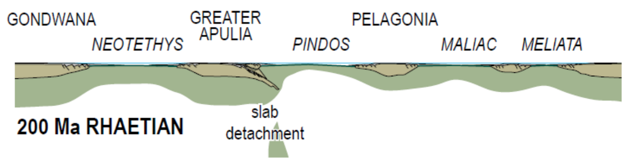	*During the Rhaetian the thermal subsidence stage of the Pindos basin continued accompanied by the deposition of the Drimos Formation. [Stampfli, 2010]*

Today, the Cimmerian fold belt is a string of folded mountains that are integrated into the Alpine Mountain belt, which stretches from the Balkans to south-east Asia and may be observed in mountain ranges across what is now Turkey, Iran, Afghanistan, Tibet, and parts of Southeast Asia. However, the Cimmerian orogeny took place more than 100 million years before Alpine Mountain building. The Cimmerian terrane split off from the northern edge of south-east Pangaea (Gondwana) in the Permian period. The fragment rotated like the hand of a clock, but anti-clockwise, around a point at its north-western end, which was located in the area of today's Carpathian Mountains. The western Cimmerian mountains contain predominantly overprinted Variscan and Cadomian crust. *[Wikipedia]*

The “Eo-Cimmerian” refers to the early phase of the Cimmerian orogeny, a mountain-building event that took place during the Late Triassic period, roughly around 230 to 200 million years ago. This phase marks the collision of the Cimmerian microcontinent with the southern margin of Eurasia. On a timeline the Late Triassic Eo-Cimmerian precedes the main Cimmerian orogeny, which continued into the Jurassic period. On a stratigraphic column an Eo-Cimmerian might be represented by the end of passive margin sedimentation and the start of compressional tectonics in a particular region.

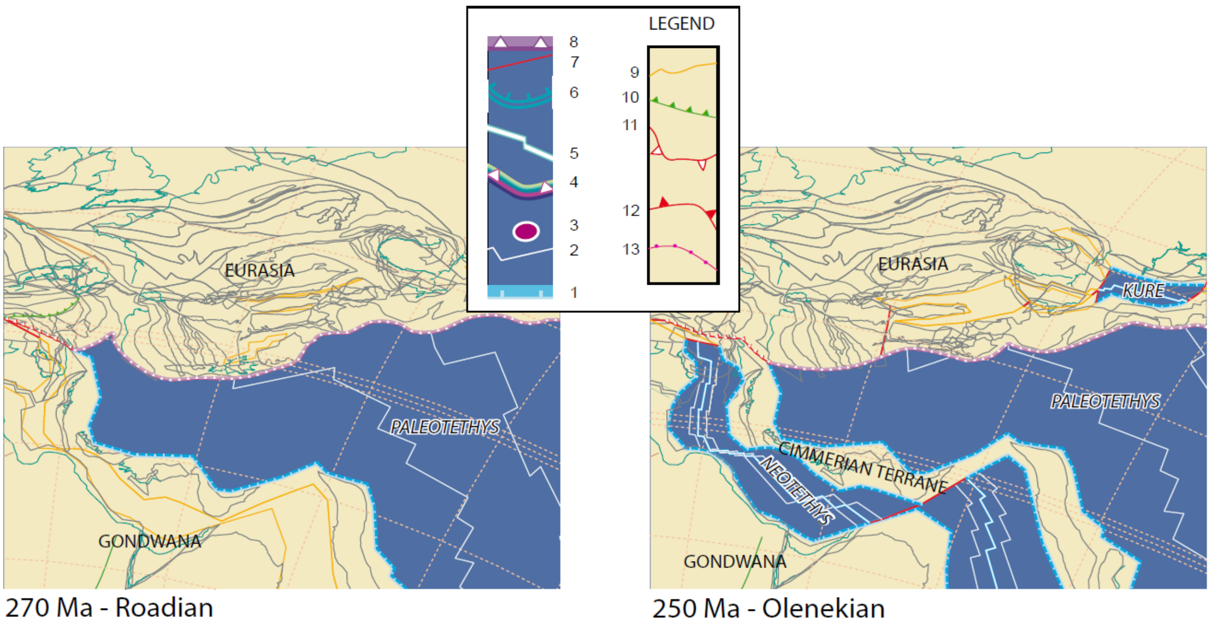

Plates tectonic model from Middle Permian to Late Triassic. modified after Stampfli & Hochard (2009) and Moix (2010). 1. passive margin; 2. magnetic anomalies or synthectic anomalies; 3. seamount; 4. intraoceanic subduction/arc complex; 5. spreading ridges; 6. obductions; 7. Transform and strike-slip faulting; 8. subduction zone; 9. rifts; 10. inversion zones; 11. collision zones; 12. activethrusts; 13. sutures. (PL = Pelagonia). The black lines represent the sections shown above

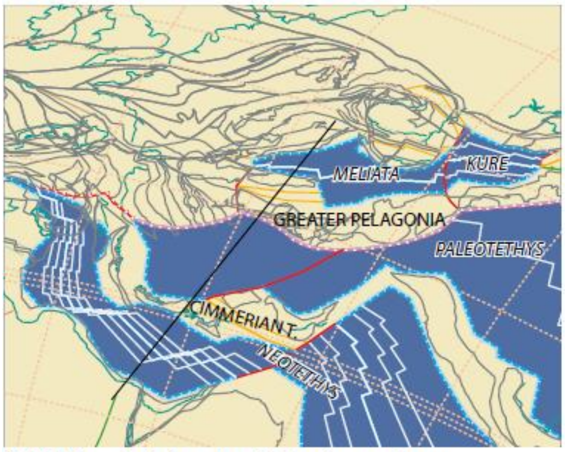

240 Ma - Anisian-Ladinian boundary

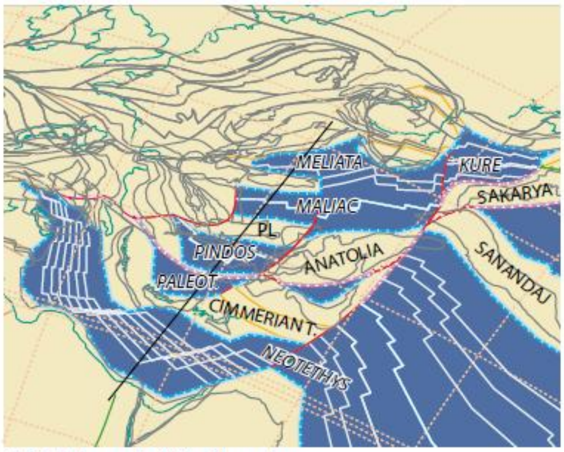

230 Ma - middle Carnian

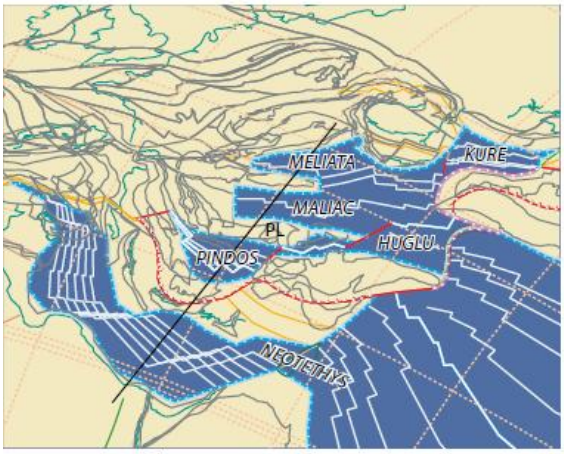

220 Ma - early Norian

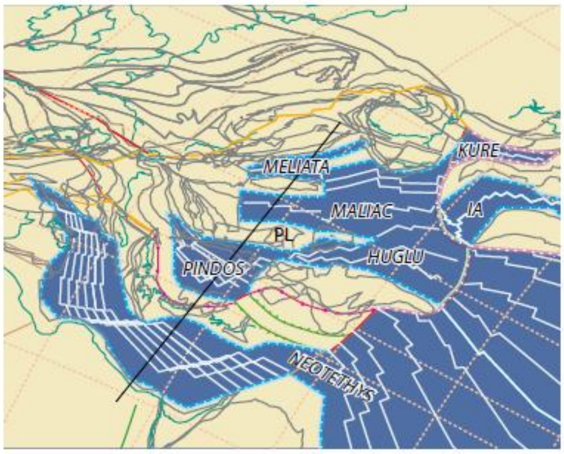

200 Ma - Rhaetian

[Source: Stampfli, 2010]

Closure of the Vadar and Pindos Basins and the Alpine Orogeny

During the Middle Jurassic the Vardar basin completely replaced the previous back-arc basins and at the same time its ridge was obducted (i.e. was pushed upwards) onto the Pelagonian microcontinent from East to West. In the late Oxfordian a new ocean ridge was formed between the Huğlu and Vardar basins. The newly formed Lycian basin was part of Vardar basin. Towards the end of Early Cretaceous, the Vardar oceanic crust was subducted northward under the Rhodope inducing the opening of the Black Sea. Simultaneously, the Huğlu subducted under the continuation of the Neothethyan trench causing the obduction of the Lycian slab in Cenomanian-Turonian time. In the East the Lycian nappes stopped at the Anatolian margin. In contrast, in the West, the Pelagonian microcontinent was significantly extended which enabled the propagation of the arc with the obduction front into the Pindos basin (subduction propagation). At the end of the Cretaceous the Vardar supra-subduction-zone (SSZ) was closed and the Pindos slab (consisting of oceanic crust) was subducted toward the East. During the Tertiary the geometry of the Hellenides underwent no major changes. After the subduction and sealing of the Pindos (ocean), the geodynamics was controlled by the Neotethyan (Eastern Mediterranean) subduction, which initiated significant extension within the whole Hellenic orogenic wedge.

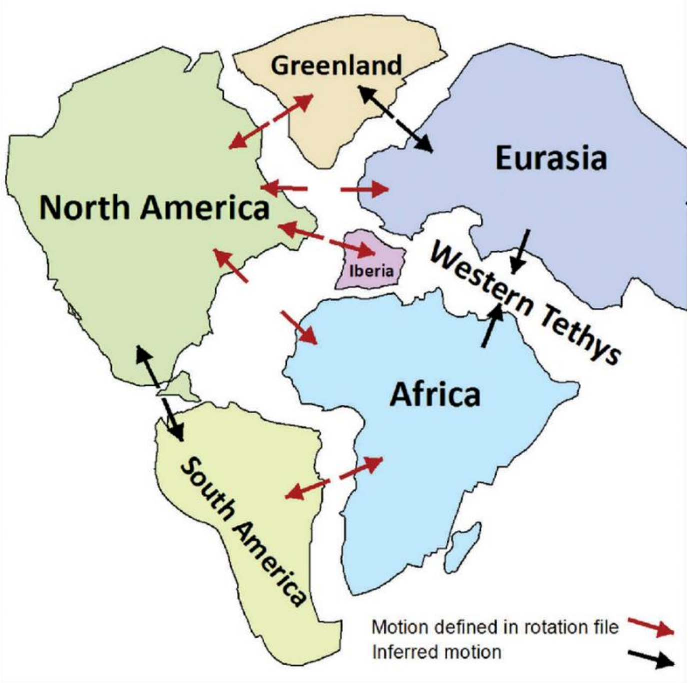

Schematic illustration of the Western Tethys region in the framework of surrounding plates from the Jurassic onwards [Hosseinpour M, et al. 2016.]

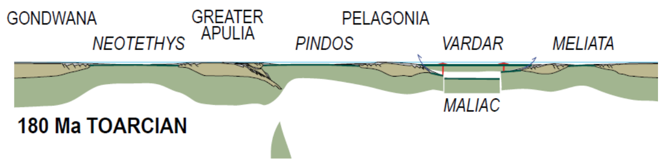	*Sedimentation into the Pindos is going on with a continuous evolution to more pelagic facies. The radiolarites mark the passage from the Drimos to the Lesteena Fm. North of Pelagonia, the Maliac subducts toward the East providing room for the supra-subduction Vardar ocean.*
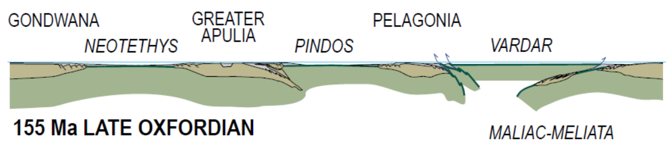	*The deep-sea Lesteena Fm is still depositing in the Pindos domain. Maliac and Meliata are completely subducted, when the Vardar ridge diachronically obducts along the Pelagonian northern margin from the East to the West, forming the largest ophiolitic belt of the Hellenides. Elements of the lower plate like oceanic seamounts or slices of the margin succession are scraped and carried with the Vardar nappe. This event causes an important flexuration marked by the deposition of Oxfordian-Kimmeridgian radiolarites.*
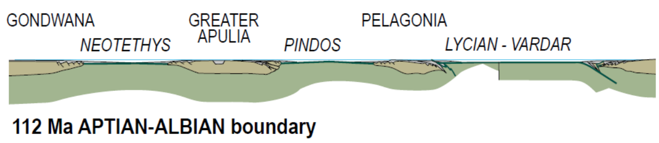	*The Lambia Fm is forming in the Pindos basin. Sediments are mostly pelagic limestones, Degnan & Robertson (1998) invoke the presence of strong current because of the reworking of intrabasinal deposits in calc-rudites and calc-arenites. North of Pelagonia, the passive margin is reset and the young Lycian ridge is spreading. The remnant Vardar oceanic floor subducts toward the North, under*

	the Rhodope, after a subduction reversal event (Bonev & Stampfli, 2003)
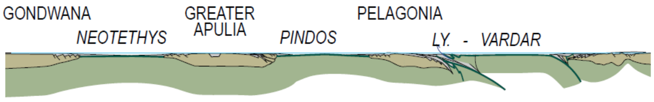 **90 Ma TURONIAN**	*The Lycian ridge is already obducting on the Eastern Pelagonian margin, picking up the Vardar ophiolites again. This event provokes the bulging of the microcontinent, which implies a partial emersion that stops the pelagic deposition. On the other hand, shallow water conditions further the development of platforms (i.e. the Arvi creamy limestones). The ophiolitic front is accompanied by an arc which constitutes a precursor of the Asteroussia s.s., propagating to the Pindos northern margin. The flexural bulge was subject to erosion, which is regarded as the source for the Pindos first flysch. Further-flexuration followed the obduction inducing the deposition of pelagic limestones Turonian to Santonian in age.*
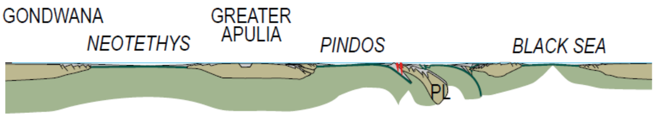 **70 Ma MAASTRICHTIAN**	*The remaining Vardar Ocean is completely subducted causing the opening of the Black Sea within the Eastern Rhodope and Pontides. Pindos subduction starts a roll-back stage inducing extension on the active margin. Stampfli suggests that the Arvi lavas that were associated with the deposition of Pindos basin red shales and pelagic limestones were emplaced in this context.* *PL = Pelagonia*
66 - 33 Ma PALEOCENE-OLIGOCENE	*During the Paleocene-Oligocene period, the Pindos slab subducts until the collision of the arc with the Greater Apulia terrane. This stage is marked by the continuous deposition of the Pindos second flysch.*

[Source: Stampfli, 2010]

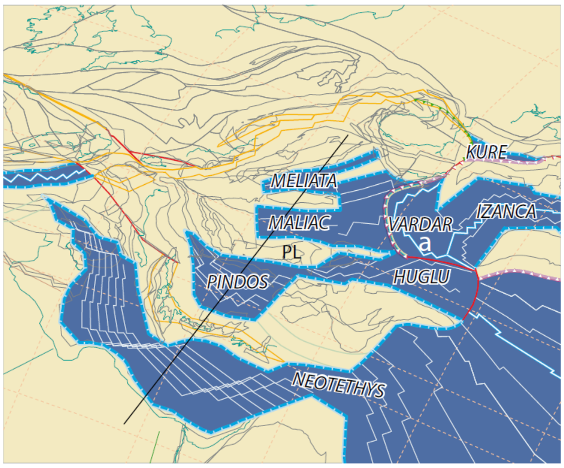

180 Ma - Toarcian

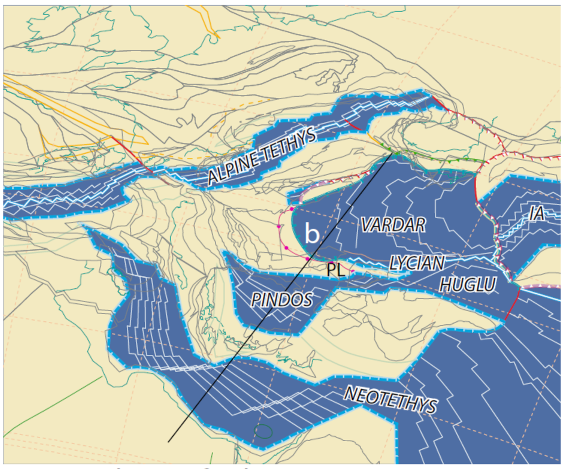

155 Ma - late Oxfordian

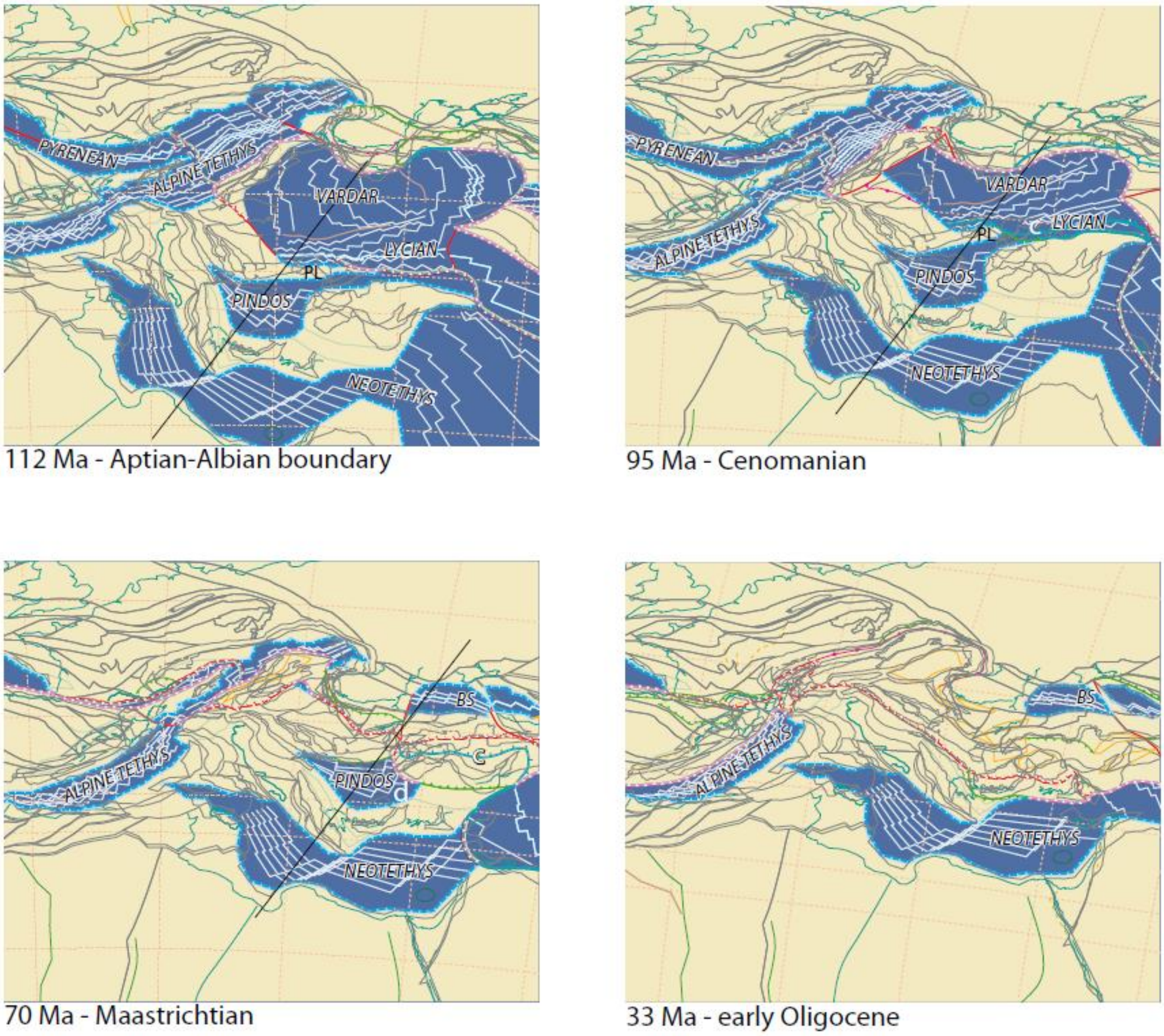

Plates tectonic model from Early Jurassic to Oligocene modified after Stampfli & Hochard (2009) and Moix (2010). ***a)*** *Vardar SSZ spreading;* ***b)*** *Vardar obduction;* ***c)*** *Lycian obduction;* ***d)*** *arc propagation into the Pindos (IA = Izmir-Ankara, BS = Black Sea).*

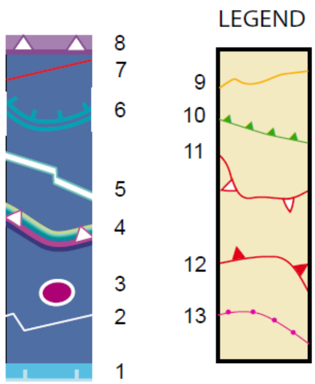

1 passive margin; 2. magnetic anomalies or synthectic anomalies; 3. seamount; 4. intraoceanic subduction/arc complex; 5. spreading ridges; 6. obductions; 7. Transform and strike-slip faulting; 8. subduction zone; 9. rifts; 10. inversion zones; 11. collision zones; 12. activethrusts; 13. sutures. (PL = Pelagonia).

[Source: Stampfli, 2010]

Uranium–lead dating

[Wikipedia]

Wikipedia
Die freie Enzyklopädie

Uranium–lead dating, abbreviated U–Pb dating, is one of the oldest and most refined of the radiometric dating schemes. It can be used to date rocks that formed and crystallised from about 1 million years to over 4.5 billion years ago with routine precisions in the 0.1–1 percent range.

The method is usually applied to zircon. This mineral incorporates uranium and thorium atoms into its crystal structure, but strongly rejects lead when forming. As a result, newly-formed zircon crystals will contain no lead, meaning that any lead found in the mineral is radiogenic. Since the exact rate at which uranium decays into lead is known, the current ratio of lead to uranium in a sample of the mineral can be used to reliably determine its age. The method relies on two separate decay chains, the uranium series from 238U to 206Pb, with a half-life of 4.47 billion years and the actinium series from 235U to 207Pb, with a half-life of 710 million years.

Decay routes

Uranium decays to lead via a series of alpha and beta decays, in which 238U and its daughter nuclides undergo a total of eight alpha and six beta decays, whereas 235U and its daughters only experience seven alpha and four beta decays. The existence of two 'parallel' uranium–lead decay routes (238U to 206Pb and 235U to 207Pb) leads to multiple feasible dating techniques within the overall U–Pb system. The term U–Pb dating normally implies the coupled use of both decay schemes in the 'concordia diagram' (see below). However, use of a single decay scheme (usually ^{238}U to ^{206}Pb) leads to the U–Pb isochron dating method, analogous to the rubidium–strontium dating method.

Finally, ages can also be determined from the U–Pb system by analysis of Pb isotope ratios alone. This is termed the lead–lead dating method. Clair Cameron Patterson, an American geochemist who pioneered studies of uranium–lead radiometric dating methods, used it to obtain one of the earliest estimates of the age of the Earth.

Mineralogy

Although zircon ($ZrSiO_4$) is most commonly used, other minerals such as monazite (see: monazite geochronology), titanite, and baddeleyite can also be used. Where crystals such as zircon with uranium and thorium inclusions cannot be obtained, uranium–lead dating techniques have also been applied to other minerals such as calcite / aragonite and other carbonate minerals. These types of minerals often produce lower-precision ages than igneous and metamorphic minerals traditionally used for age dating, but are more commonly available in the geologic record.

Mechanism

During the alpha decay steps, the zircon crystal experiences radiation damage, associated with each alpha decay. This damage is most concentrated around the parent isotope (U and Th), expelling the daughter isotope (Pb) from its original position in the zircon lattice. In areas with a high concentration of the parent isotope, damage to the crystal lattice is quite extensive, and will often interconnect to form a network of radiation damaged areas. Fission tracks and micro-cracks within the crystal will further extend this radiation damage network. These fission tracks act as conduits deep within the crystal, providing a method of transport to facilitate the leaching of lead isotopes from the zircon crystal.

Computation

Under conditions where no lead loss or gain from the outside environment has occurred, the age of the zircon can be calculated by assuming exponential decay of uranium. That is

$$N_{\mathrm{n}} = N_{\mathrm{o}} e^{-\lambda t}$$

where

- $N_{\mathrm{n}} = \mathrm{U}$ is the number of uranium atoms measured now.
- N_{o} is the number of uranium atoms originally - equal to the sum of uranium and lead atoms $\mathrm{U} + \mathrm{Pb}$ measured now.
- $\lambda = \lambda_{\mathrm{U}}$ is the decay rate of Uranium.
- t is the age of the zircon, which one wants to determine.

This gives

$$\mathrm{U} = (\mathrm{U} + \mathrm{Pb})\, e^{-\lambda_{\mathrm{U}} t},$$

which can be written as

$$\frac{\mathrm{Pb}}{\mathrm{U}} = e^{\lambda_{\mathrm{U}} t} - 1.$$

The more commonly used decay chains of Uranium and Lead gives the following equations:

$$\frac{{}^{206}\mathrm{Pb}^*}{{}^{238}\mathrm{U}} = e^{\lambda_{238} t} - 1, \qquad \textbf{(1)}$$

$$\frac{{}^{207}\mathrm{Pb}^*}{{}^{235}\mathrm{U}} = e^{\lambda_{235} t} - 1. \qquad \textbf{(2)}$$

(The notation Pb^*, sometimes used in this context, refers to *radiogenic* lead. For zircon, the *original* lead content can be assumed to be zero, and the notation can be ignored.) These are said to yield concordant ages (*t* from each equation 1 and 2). It is these concordant ages, plotted over a series of time intervals, that result in the concordant line. *[Wikipedia]*

Oolite

WIKIPEDIA
Die freie Enzyklopädie

Oolite is a sedimentary rock formed from ooids, spherical grains composed of concentric layers. Strictly, oolites consist of ooids of diameter 0.25–2 millimetres; rocks composed of ooids larger than 2 mm are called pisolites. The term oolith can refer to oolite or individual ooids. *[Wikipedia]*

Modern ooids from a beach on Joulter Cays, The Bahamas

Thin-section of calcitic ooids from an oolite within the Carmel Formation (Middle Jurassic) of southern Utah

Ooids are most commonly composed of calcium carbonate (calcite or aragonite), but can be composed of phosphate, clays, chert, dolomite or iron minerals, including hematite. Dolomitic and chert ooids are most likely the result of the replacement of the original texture in limestone.

They are usually formed in warm, supersaturated, shallow, highly agitated marine water intertidal environments, though some are formed in inland lakes. The mechanism of formation starts with a small fragment of sediment acting as a 'seed', such as a piece of a shell. Strong intertidal currents wash the 'seeds' around on the seabed, where they accumulate layers of chemically precipitated calcite from the supersaturated water. The oolites are commonly found in large current bedding structures that resemble sand dunes. The size of the oolites reflect the time that they were exposed to the water before they were covered with later sediment. *[Wikipedia]*

Oncoids

Paleoproterozoic oncoids from the Franceville Basin, Gabon, Central Africa. Oncoids are unfixed stromatolites ranging in size from a few millimeters to a few centimeters

Stromatolites

https://www.wikiwand.com/en/Stromatolite

Stromatolites are layered sedimentary formations that are created mainly by photosynthetic microorganisms such as cyanobacteria, sulfate-reducing bacteria, and Pseudomonadota (formerly proteobacteria). These microorganisms produce adhesive compounds that cement sand and other rocky materials to form mineral "microbial mats". In turn, these mats build up layer by layer, growing gradually over time. A stromatolite may grow to a meter or more. Fossilized stromatolites provide important records of some of the most ancient life. As of the Holocene, living forms are rare.

Modern stromatolites in Shark Bay, Western Australia

Morphology

Fossilized stromatolites, about 425 million years old, in the Soeginina Beds (Paadla Formation, Ludlow, Silurian) near Kübassaare, Estonia

Stromatolites are layered, biochemical, accretionary structures formed in shallow water by the trapping, binding and cementation of sedimentary grains in biofilms (specifically microbial mats), through the action of certain microbial lifeforms, especially cyanobacteria. They exhibit a variety of forms and structures, or morphologies, including conical, stratiform, domal, columnar, and branching types. Stromatolites occur widely in the fossil record of the Precambrian, but are rare today. Very few Archean stromatolites contain fossilized microbes, but fossilized microbes are sometimes abundant in Proterozoic stromatolites.

While features of some stromatolites are suggestive of biological activity, others possess features that are more consistent with abiotic (non-biological) precipitation. Finding reliable ways to distinguish between biologically formed and abiotic stromatolites is an active area of research in geology. Be it as it may, multiple morphologies of stromatolites may exist in a single local or geological stratum, relating to the specific conditions occurring in different region and water depths.

Most stromatolites are spongiostromate in texture, having no recognisable microstructure or cellular remains. A minority are porostromate, having recognisable microstructure; these are mostly unknown from the Precambrian but persist throughout the Palaeozoic and Mesozoic. Since the Eocene, porostromate stromatolites are known only from freshwater settings. *[Wikipedia]*

Formation

Time lapse photography of modern microbial mat formation in a laboratory setting gives some revealing clues to the behavior of cyanobacteria in stromatolites. Biddanda et al. (2015) found that cyanobacteria exposed to localized beams of light moved towards the light, or expressed phototaxis, and increased their photosynthetic yield, which is necessary for survival. In a novel experiment, the scientists projected a school logo onto a petri dish containing the organisms, which accreted beneath the lighted region, forming the logo in bacteria. The authors speculate that such motility allows the cyanobacteria to seek light sources to support the colony. In both light and dark conditions, the cyanobacteria form clumps that then expand outwards, with individual members remaining connected to the colony via long tendrils. This may be a protective mechanism that affords evolutionary benefit to the colony in harsh environments where mechanical forces act to tear apart the microbial mats. Thus these sometimes elaborate structures, constructed by microscopic organisms working somewhat in unison, are a means of providing shelter and protection from a harsh environment.

Lichen stromatolites are a proposed mechanism of formation of some kinds of layered rock structure that are formed above water, where rock meets air, by repeated colonization of the rock by endolithic lichens. *[Wikipedia]*

Fossil record

Some Archean rock formations show macroscopic similarity to modern microbial structures, leading to the inference that these structures represent evidence of ancient life, namely stromatolites. However, others regard these patterns as being due to natural material deposition or some other abiogenic mechanism. Scientists have argued for a biological origin of stromatolites due to the presence of organic globule clusters within the thin layers of the stromatolites, of aragonite nanocrystals (both features of current stromatolites), and of other microstructures in older stromatolites that parallel those in younger stromatolites that show strong indications of biological origin.

Fossilized stromatolites in the Hoyt Limestone (Cambrian) exposed at Lester Park, near Saratoga Springs, New York

Fossilized stromatolites (Pika Formation, middle Cambrian) near Helen Lake, Banff National Park, Canada

Stromatolites are a major constituent of the fossil record of the first forms of life on earth. They peaked about 1.25 billion years ago and subsequently declined in abundance and diversity, so that by the start of the Cambrian they had fallen to 20% of their peak. The most widely supported explanation is that stromatolite builders fell victim to grazing creatures (the Cambrian substrate revolution); this theory implies that sufficiently complex organisms were common over 1 billion years ago. Another hypothesis is that protozoans such as foraminifera were responsible for the decline, favoring formation of thrombolites over stromatolites through microscopic bioturbation.

Proterozoic stromatolite microfossils (preserved by permineralization in silica) include cyanobacteria and possibly some forms of the eukaryote chlorophytes (that is, green algae). One genus of stromatolite very common in the geologic record is Collenia.

The connection between grazer and stromatolite abundance is well documented in the younger Ordovician evolutionary radiation; stromatolite abundance also increased after the end-Ordovician and end-Permian extinctions decimated marine animals, falling back to earlier levels as marine animals recovered. Fluctuations in metazoan population and diversity may not have been the only factor in the reduction in stromatolite abundance. Factors such as the chemistry of the environment may have been responsible for changes.

While prokaryotic cyanobacteria reproduce asexually through cell division, they were instrumental in priming the environment for the evolutionary development of more complex eukaryotic organisms. They are thought to be largely responsible for increasing the amount of oxygen in the primeval Earth's atmosphere through their continuing photosynthesis (see Great Oxygenation Event). They use water, carbon dioxide, and sunlight to create their food. A layer of polysaccharides often forms over mats of cyanobacterial cells. In modern microbial mats, debris from the surrounding habitat can become trapped within the polysaccharide layer, which can be cemented together by the calcium carbonate to grow thin laminations of limestone. These laminations can accrete over time, resulting in the banded pattern common to stromatolites. The domal morphology of biological stromatolites is the result of the vertical growth necessary for the continued infiltration of sunlight to the organisms for photosynthesis. Layered spherical growth structures termed oncolites are similar to stromatolites and are also known from the fossil record. Thrombolites are poorly laminated or non-laminated clotted structures formed by cyanobacteria, common in the fossil record and in modern sediments. There is evidence that thrombolites form in preference to stromatolites when foraminifera are part of the biological community.

The Zebra River Canyon area of the Kubis platform in the deeply dissected Zaris Mountains of south western Namibia provides an extremely well exposed example of the thrombolite-stromatolite-metazoan reefs that developed during the Proterozoic period, the stromatolites here being better developed in updip locations under conditions of higher current velocities and greater sediment influx. *[Wikipedia]*

Crinoids

KU | Kansas Geological Survey
GeoKansas
HOME / ROCKS, MINERALS, AND FOSSILS / FOSSILS IN KANSAS / INVERTEBRATE FOSSILS IN KANSAS

Text and photos from "Windows to the Past: A Guidebook to Common Invertebrate Fossils of Kansas", Kansas Geological Survey Educational Series 16. Crinoids | GeoKansas

Stratigraphic Range: Ordovician (or possibly Middle Cambrian) to Holocene. Taxonomic Classification: Crinoids belong to the Kingdom Animalia, Phylum Echinodermata, Subphylum Crinozoa, Class Crinoidea.

Because many crinoids resemble flowers, with their cluster of waving arms atop a long stem, they are sometimes called sea lilies. But crinoids are not plants. Like their relatives—starfishes, sea urchins, sea cucumbers, and brittle stars—crinoids are echinoderms, animals with rough, spiny surfaces and a special kind of radial symmetry based on five or multiples of five.

Crinoids have lived in the world's oceans since at least the beginning of the Ordovician Period, roughly 485 million years ago.

Crinoids flourished during the Paleozoic Era, carpeting the seafloor like a dense thicket of strange flowers, swaying this way and that with the ocean currents. They peaked during the Mississippian subperiod, when the shallow, marine environments they preferred were widespread on several continents. Massive limestones in North America and Europe, made up almost entirely of crinoid fragments, attest to the abundance of these creatures during the Mississippian.

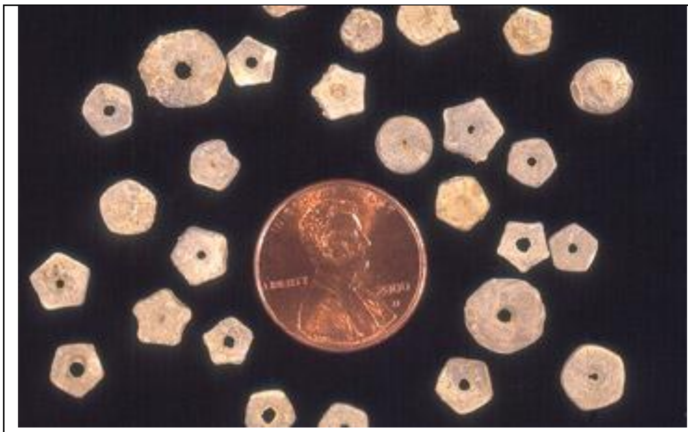

Individual stem pieces are common fossils in Kansas rocks. These samples of different Pennsylvanian crinoid species are from the Spring Branch Limestone Member, Lecompton Limestone, Greenwood County.

Uintacrinus socialis is a stemless crinoid that lived in the shallow Cretaceous seas that covered much of North America roughly 70 million years ago. Among the numerous arms preserved in the top photo, a segmented calyx is also visible. These specimens were collected from the Niobrara Chalk, Gove County. In this close-up of another specimen (lower photo), the individual arm segments are easy to see.

Crinoids came close to extinction toward the end of the Permian Period, about 252 million years ago. The end of the Permian was marked by the largest extinction event in the history of life. The fossil record shows that nearly all the crinoid species died out at this time. The one or two surviving lineages eventually gave rise to the crinoids populating the oceans today.

Based on the fossil record of crinoids, especially the details of the plates that made up the arms and calyx, experts have identified hundreds of different crinoid species. Though most crinoids had stems, not all did. Today, stemless crinoids live in a wide range of ocean environments, from shallow to deep, whereas their relatives with stems normally live only at depths of 300 feet or more. These modern crinoids are an important source of information about how the many different extinct crinoids lived.

Rarely are crinoids preserved in their entirety: once the soft parts of the animal decayed, sea currents generally scattered the skeletal segments. By far the most common crinoid fossils are the stem pieces. Only occasionally is the cuplike calyx found.

KU Kansas Geological Survey
GeoKansas

HOME / ROCKS, MINERALS, AND FOSSILS / FOSSILS IN KANSAS / INVERTEBRATE FOSSILS IN KANSAS

Brachiopods (Protozoic, Kansas)

Text and photos from "Windows to the Past: A Guidebook to Common Invertebrate Fossils of Kansas", Kansas Geological Survey Educational Series 16. [*Brachiopods | GeoKansas*]

Taxonomic Classification: Brachiopods belong to Kingdom Animalia, Phylum Brachiopoda. The phylum is divided into three subphyla, the Linguliformea, Craniiformea, and Rhynchonelliformea. Stratigraphic Range: Lower Cambrian to Holocene.

Brachiopods are marine animals that secrete a shell consisting of two parts called valves. They have an extensive fossil record, first appearing in rocks dating back to the early part of the Cambrian Period, about 541 million years ago. They were extremely abundant during the Paleozoic Era, reaching their highest diversity roughly 400 million years ago, during the Devonian Period. At the end of the Paleozoic, however, they were decimated in the mass extinction that marks the end of the Permian Period, about 252 million years ago. Although some brachiopods survived and their descendants live in today's oceans, they never achieved their former abundance and diversity. Only about 300 to 500 species of brachiopods exist today, a small fraction of the perhaps 15,000 species (living and extinct) that make up the phylum Brachiopoda.

Brachiopods commonly found in Kansas rocks (Carboniferous to Permian): Neospirifer, Farley Limestone Member, Wyandotte Limestone, Johnson County; Meekella, collected near Beaumont, Butler County; Derbyia, Speiser Shale, Council Grove Group, Cowley County; Crurythyris, Beil Limestone Member, Lecompton Limestone, Douglas County; Phricodothyris, Lecompton Limestone,Douglas County; Neochonetes, Garrison Shale, Council Grove Group, Riley County; Hustedia, Topeka Limestone, Shawnee Group, Jefferson County.

Exceptionally preserved brachiopod fossil (center, note delicate spines still attached to the valve) collected from Coal Creek Limestone Member, Topeka Limestone, near Topeka

Brachiopod shells come in a variety of shapes and sizes. Sometimes the bottom valve is convex like the top valve, but in many species the bottom valve is concave or occasionally conical. In some brachiopods, the top valve is concave and the bottom is convex. The outer surface of the valves may be marked by concentric wrinkles or radial ribs. Some brachiopods have prominent spines, but usually these are broken off and are found as separate fossils.The shells of living brachiopods typically range in size from less than 0.25 inches to just over 3 inches in length or width. Fossil brachiopods generally fall within this same range, though some adults have shells that are less than 0.04 inches in diameter, and an exceptional few have shells that are 15 inches across.

Most brachiopods live in relatively shallow marine water, up to about 650 feet (200 m), but some species have been found at depths of more than a mile. Because many fossils species are found in shales, which form from deposits of mud and silt, we know that some brachiopod species thrived in muddy environments.

Because of their worldwide abundance, diversity, and rapid evolution in the Paleozoic, brachiopod fossils are useful indicators of the ages of different rock layers. By matching the brachiopod species contained within rocks deposited in different locations, paleontologists can determine that the rock units were deposited at the same time.

KU Kansas Geological Survey GeoKansas

HOME / ROCKS, MINERALS, AND FOSSILS / FOSSILS IN KANSAS / INVERTEBRATE FOSSILS IN KANSAS

Corals

Text and photos from "Windows to the Past: A Guidebook to Common Invertebrate Fossils of Kansas", Kansas Geological Survey Educational Series 16. [Corals | GeoKansas]

Corals are simple animals that secrete skeletons made of calcium carbonate. They are close relatives of sea anemones and jellyfish and are the main reef builders in modern oceans. Corals can be either colonial or solitary.

As fossils, corals are found worldwide in sedimentary rocks. Based on these fossils, we know that the corals began their long evolutionary history in the Middle Cambrian, more than 510 million years ago. Modern corals inhabit deep-water environments as well as shallow reefs. Based on evidence from the rocks, scientists have determined that corals lived in warm, shallow, sunlit waters where the bottom was firm enough to offer a secure point of attachment.

Two groups of corals were important inhabitants of the Pennsylvanian and Permian seas—tabulate and rugose corals. Tabulate corals were exclusively colonial and produced calcium carbonate skeletons in a variety of shapes: moundlike, sheetlike, chainlike, or branching. Tabulate corals get their name from horizontal internal partitions known as tabulae. Some tabulate corals were probably reef builders.

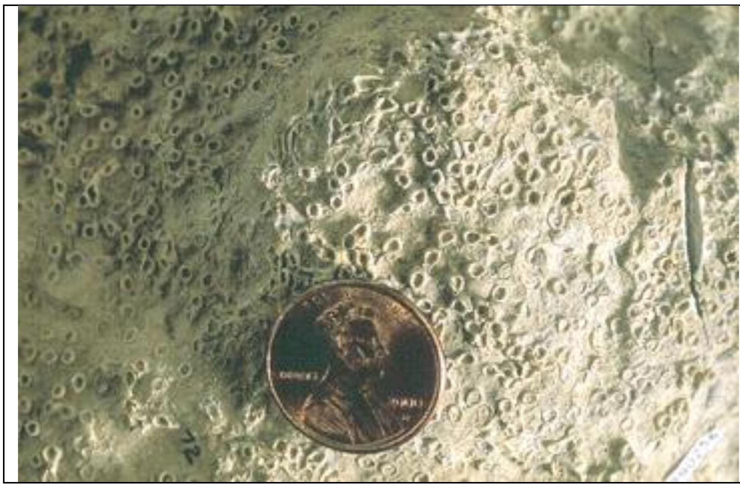

This sample of the colonial coral Cladochonus is from the Beil Limestone Member, Lecompton Limestone, Greenwood County (Kansas). This limestone was deposited during the Pennsylvanian Subperiod, about 300 million years ago.

A common characteristic of rugose corals, from which they get their name, is the wrinkled appearance of their outer surface. (Rugose comes from the Latin word for wrinkled.) Rugose corals may be either solitary or colonial. Because solitary rugose corals are commonly shaped like a horn, these fossils are sometimes called horn corals.

Both tabulate and rugose corals died out in the major extinction that occurred at the end of the Permian Period, roughly 252 million years ago. This extinction marked the end of the Paleozoic Era. The corals that inhabited the post-Paleozoic seas differ significantly from the earlier corals. Because of this, many specialists argue that these later corals may not be closely related to the Paleozoic corals.

Text and photos from "Windows to the Past: A Guidebook to Common Invertebrate Fossils of Kansas", Kansas Geological Survey Educational Series 16. https://www.kgs.ku.edu/geokansas/

Fossils in Thin Section

Page Quinton via Wikimedia Commons; CC BY-SA 4.0

The following diagrams show schematic representations of some of the most common fossils encountered in thin sections; they are not organized taxonomically, but rather based on gross morphology. Please note that the scale bar in the following four diagrams is approximate and that the actual sizes of the fossils can vary by an order of magnitude or more.

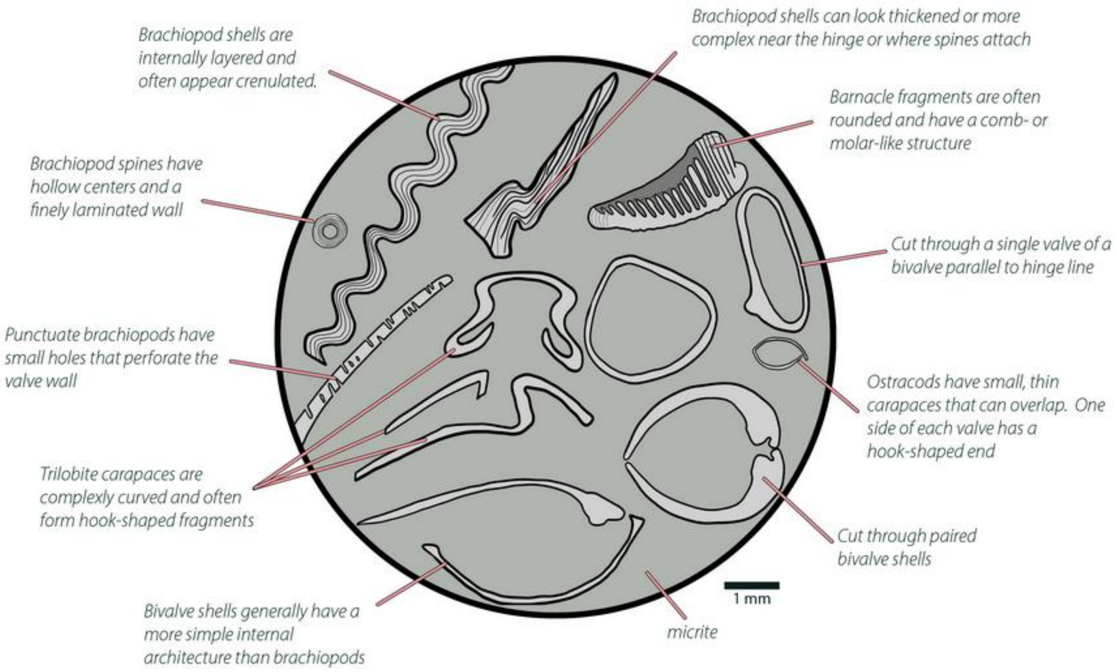

Fossils that are, or appear to be, made out of a walled shell or exoskeleton include brachiopods, bivalves, barnacles, and trilobites (Page Quinton via Wikimedia Commons; CC BY-SA 4.0) [Source: Sedimentary Geology: Rocks, Environments and Stratigraphy, Michael Rygel and Page Quinton SUNY Potsdam, https://geo.libretexts.org/Courses/SUNY_Potsdam/Sedimentary_Geology%3A_Rocks_Environments_and_Stratigraphy/09%3A_Fossils/9.7%3A_Fossils_in_Thin_Section#Crinoids]

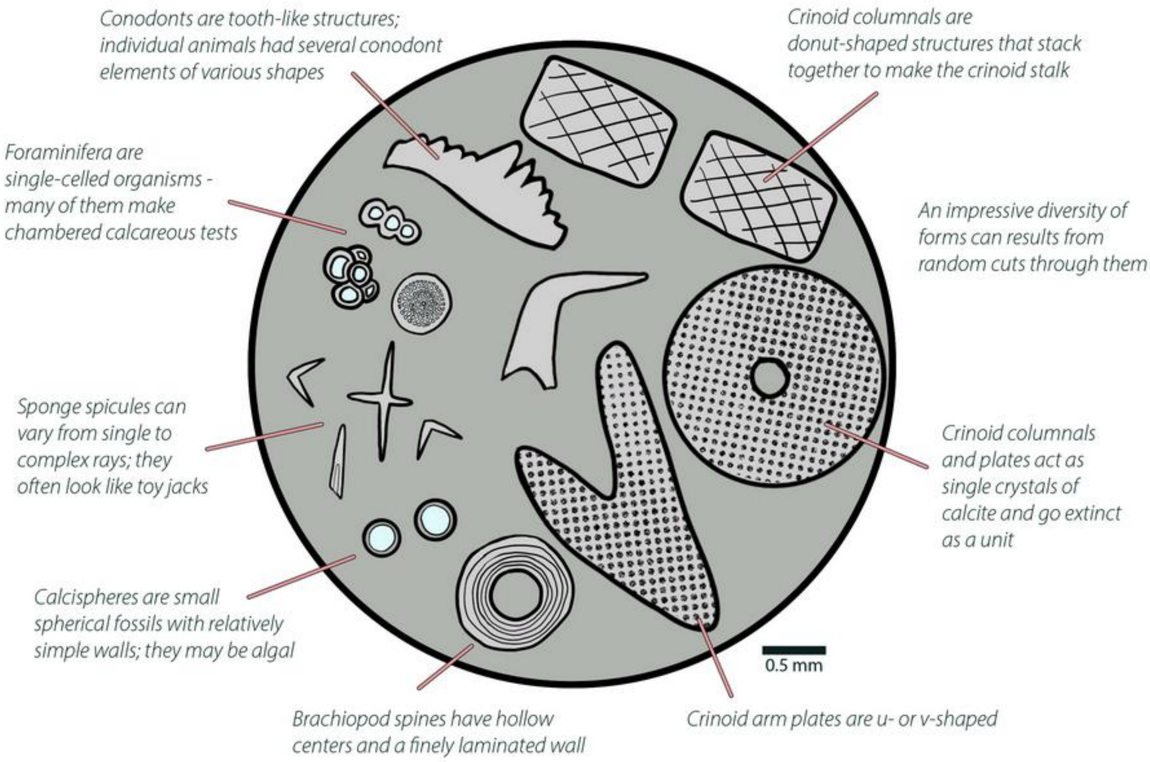

Figure 9.7.4*: Other distinctive or noteworthy fossils encountered in thin section include crinoid plates, crinoid columnals, brachiopod spines, calcispheres, sponge spicules, and conodonts (Page Quinton via Wikimedia Commons;* CC BY-SA 4.0*). [Source: Sedimentary Geology: Rocks, Environments and Stratigraphy, Michael Rygel and Page Quinton SUNY Potsdam]*